# EFFECT OF BROWN'S GAS ENRICHED HYDROCARBON COMBUSTION

# ON ENGINE EMISSIONS AND PERFORMANCE

**By**

**J. Lalnunthari**

**Physics Department**

**Submitted in partial fulfillment for the requirement of the Degree of Doctor of Philosophy in Physics of Mizoram University, Aizawl**

I, J. Lalnunthari, a Ph.D scholar in Physics Department, Mizoram University, do hereby declare that the subject matter of this thesis is the record of work done by me, that the contents of this thesis did not form basis of the award of any previous degree to me or to the best of my knowledge to anybody else, and that the thesis has not been submitted by me for any research degree in any other University/Institute.

This thesis is being submitted to Mizoram University for the degree of Doctor of Philosophy in Physics.

<div align="right">

**(J. LALNUNTHARI)**

**Candidate**

</div>

**(Prof. R.C Tiwari)**                                    **(Dr. HRANGHMINGTHANGA)**

**Head**                                                          **Supervisor**

Dr. Hranghmingthanga
Assistant Professor

Department of Physics
Mizoram University
Tanhril-796004

Aizawl, Mizoram

**MIZORAM UNIVERSITY**
**DEPARTMENT OF PHYSICS**
**AIZAWL 796 004 MIZORAM**
Phones: 0389 - 2330522
FAX : 0389 - 2330522
Mobile: +919436141509
E-mail: hthanga@yahoo.com

**(A Central University Established by an Act of Parliament)**

**Date: 23rd January, 2019**

*Certificate*

*This is to certify that the thesis entitled Effect of Brown's Gas Enriched Hydrocarbon Combustion on Engine Emissions and Performance submitted by Ms. J. Lalnunthari, for the degree of Doctor of Philosophy in Physics, of the Mizoram University: Aizawl, India, embodies the record of original investigations carried out by her under my supervision. She has been duly registered and the thesis presented is worthy of being considered for the award of Ph.D. degree. This research work has not been submitted for any degree of any other university.*

**(Dr. Hranghmingthanga)**

**Supervisor**

*Acknowledgement*

---

After an intensive study of few years, I finally reached the finishing touch of my Ph.D dissertation. I would like to express my sincere gratitude to all those who helped me throughout the whole period of my research.

First of all, I would like to thank my supervisor Dr. Hranghmingthanga for giving me the opportunity to complete my Ph.D research work under his supervision; without which I would not have completed this challenging research work. Thank you for giving me an opportunity to explore the world of Fuel Energy and meet people I would have never come across in my life; I treasure the experience and discussions in the forum. I also appreciate his devotion, ever helping hand, technical inputs and knowledge shared with me, which will always have a big impact in my future career.

I also would like to extend my special thanks to the faculty of the Department of Physics, Mizoram University for their kind valuable help at various phases of my research. I express my sincere thanks to Prof. Zaithanzauva Pachuau (DEAN, SPS), Prof. R.C. Tiwari, Prof. Suman Rai (Head, Department of Physics), Prof. R.K. Thapa, Dr. B. Lalremruata and Dr. Lalthakimi Zadeng for their encouraging words and support extended towards me. My heartfelt thanks also go to all the non-teaching staff of the Department of Physics, Mrs. Nunpuii, Mr. Mala, Mr. Ngaia and Miss. Luri.

My acknowledgement will never be completed without special mention to my friends  Mamawia, Remruata, Dr. Rebecca, Dr. Andrew, Biaktluanga, Ramnghaka,

Sangtea, Dr. VB, Dr. Rini and Dr. Achhingi for their kind support. We were not only able to support each other by deliberating over our problems and findings, but also happily talking about things other than just our works.

I am extremely thankful to my family, who meant the world to me. I treasured the support, prayers, endless love, encouragement and help rendered to me in every phase of my personal and academic life without which the completion of my work would not have been possible. I give thanks to my dearest my Mom, who is always there for me. I would also like to thank my sister J and my brother David for all the love and supports they had bestowed upon me. I consider myself the luckiest to have such an understanding and supportive family.

Most importantly, I would like to thank Almighty God for giving me good health and strength to be able to complete my research work.

Dated: 23$^{rd}$ January, 2019 (J. Lalnunthari)

Mizoram University Department of Physics

Mizoram University

Aizawl, Mizoram

# CONTENTS

## List of Figures

## List of Tables

# *Dedication*

*This work is dedicated to my Mom, Brother and Sister. I also dedicated this work especially to my Dad and Brother, may your souls shine bright in Heaven.*

# CHAPTER 1
# INTRODUCTION

# 1. INTRODUCTION

Fossil fuels have been the primary source of energy used in the world for several decades. These fuels are used for applications such as electrical power generation, heating and transportation. Even though the application of fossil fuel as fuel dates back as far as 1000 B.C., it was only after the arrival of the Industrial Revolution during mid-1700 through 1800 that coal was used as the primary source of fuel rather than biomass. The discovery of oil wells in 1859 at Titusville, Pennsylvania by Colonel Edwin Drake and subsequent development of petroleum industry marks a new era for hydrocarbon fuels as source of energy. The invention of the automobile in the early 20th century leads to exponential growth in the consumption of hydrocarbon fuels. Steam powered automobile are gradually replaced by gasoline operated vehicles (Eric, 2012). Future expansion in energy is predominant in the field of transportation where 95 percent of the fuel demands in motorization will have to be supplied by fossil fuels (Dunn, 2002). In the 21st century, the fossil fuel consumption accounts for 82% of the global energy supply, while the rest is contributed by Biofuel/waste (10%), Nuclear (5%), Hydro (2%) and the remaining 1% from other conventional source (Dincer , 2015). However, the used of hydrocarbon fuels leads to several very serious side effects (Wang *et al.*, 2012). These negative side effects include emissions of harmful polluting gases like carbon dioxides ($CO_2$), nitrogen oxides (NOx), hydrocarbons (HC), and many volatile organic compounds, some of which are known carcinogens and particulate matter (PM) (Abdel, 1988).

*Introduction*

In India road transportation sector is the single largest contributor to air pollution (Goyal, 2006). In most of Indian cities, the contribution of transport sector to the environmental pollution is estimated to be as high as 70% (Goyal, 2006; Shrivastava, 2013). Among these, carbon monoxide (CO) is the major pollutant coming from the transport sector, followed by HC and NOx (Shrivastava, 2013; Sood, 2012). Hydrocarbons react with nitrogen dioxide and sunlight and form ozone, which is beneficial in the upper atmosphere but harmful at ground level (Sood, 2012). Ozone inflames lungs, causing chest pains and coughing and making it difficult to breathe (Shrivastava, 2013). Carbon monoxide, another exhaust gas, is particularly dangerous to infants and people suffering from heart disease as it interferes with the blood's ability to transport oxygen. One of the measures taken worldwide to reduce vehicle exhaust emission is to reformulated petroleum fuel incompliance with existing emission standard. In India, Bureau of Indian Standards (BIS) notifies the required specifications for gasoline and diesel to meet the minimum requirements of Indian emission standard called Bharat stage (BS).

Bharat stage is the emission standard instituted by the Government of India to regulate the output of air pollutants from internal combustion engine from motor vehicles. At present the most prevailing emission standards are BS-III and BS-IV. To meet these emission standards two qualities of petrol are available in India, namely Normal and Xtra-premium or equivalent. In Mizoram, BS-III is the minimum emission standard that has to be met by all kind of vehicles.

Apart from this, hydrocarbon-based fuels are under limited reserves and on the verge of reaching their peak production. At the present rate of consumption, hydrocarbon fuels reserves are estimated to be depleted in less than five decades

(Sheehan *et. al.*, 1998). The continuous extensive used of hydrocarbon fuels leads to sustained high oil prices that brought about discussion of peak fuel and the potential inability of fuel production to meet the pressures of steadily growing demand. However, due to the widespread dependence on hydrocarbon fuels, it is not economically feasible to completely eliminate their use in the near future. Hence, methods are needed to significantly reduce the harmful emissions and consumption of hydrocarbon fuels.

One of the promising candidates as an alternative to fossil fuel is hydrogen. Hydrogen is the lightest chemical element with the symbol H and having molecular formula $H_2$. It is a carbon-free non-polluting, recyclable and renewable fuel. It is a sustainable form of energy as such it could solve many of the problems associated with fossil fuel due to i) its ability to burn cleanly with only water as its by-product ii) possibility of production from renewable energy source (Steinfeld, 2002) iii) its ability to work in fuel cells (Granovskii *et al.*, 2006; Kreuter *et al.*, 1998) (iv) storage in different form such gaseous, liquid, or solid in metal hydrides; (v) long distance transportation; (vi) ease of conversion to other forms of energy (vii) abundance on the planet than most of the conventional fossil fuels (Dincer, 2015). The other important advantage is that the modern SI engines can directly use hydrogen as fuel without much engine modification. However, in spite of these benefits, the present high cost of hydrogen production, storage and safety measures are the major obstacles that prevent the application of hydrogen as the main source of energy fuel compare to fossil fuel at the commercial level.

In spite of the above drawbacks addition of hydrogen gas as fuel supplement in internal combustion (IC) engines has been shown to have various beneficial

effects according to a number of studies. These effects include improvement in engine performance such as engine torque, specific fuel consumption (SFC), brake thermal efficiency and engine emissions characteristics (Cassidy, 1977; Subramanian *et al.*, 2018). The main attributes to these improvements is the better combustion characteristics of the fuel in the presence of hydrogen gas. The properties of hydrogen gas that help in the fuel combustion inside the cylinder are believe to be a) high diffusivity (0.63 cm$^2$/s, more diffusive than air by 4 times and gasoline by 12 times) b) high flame speed (270 cm/s) and c) wide flammability limits (0.1≤ $\phi$ ≤7.1) (Balat M., 2008). However, the amount of improvements achieved varies widely depending on the type of engine, fuel and method of engine optimization. In almost all the reports, addition of hydrogen in both SI and CI is shown to improve the engine torque (Yilmaz *et al.*, 2010; Andrea *et al.*, 2004). However, Sopena *et al.* reported that in pure hydrogen engine, the low volume density of hydrogen reduces the torque output as compared to pure gasoline engine (Sopena *et al.*, 2010).When hydrogen enriched fuel is used in gasoline SI engines, the observed reduction in specific fuel consumption varies from 20% to 40% according to previous studies (Dulger, 2000; Musmar, 2011; Milind *et al.*, 2011). In diesel operated engines the improvement is found to be much lesser and reach maximum around 13% after hydrogen enrichment (Yilmaz *et al.*, 2010; Wang *et al.*, 2012). The specific fuel consumption is found to decrease with increase in hydrogen percentage and reaches a certain maximum limit beyond which hydrogen loses its benefits as an additive and behaves as ordinary fuel (Bari, 2010). Hydrogen blended fuel also increases the brake thermal efficiency and according to our literature survey the improvement in brake thermal efficiency varied from 2–53% depending on the type of engine,

electrolytes used and other conditions (Ganesh *et al.*, 2008; Edward *et al.*, 2003; Ceviz *et al.*; Ji, 2009; Sharma *et al.*, 2015; Bahng *et al.*, 2016; Tamer, 2018). In most experimental research on diesel engine, an increase in break thermal efficiency was reported, while Birtas and Chiriac report a slight decrease in the brake thermal efficiency (Yilmaz *et al.*, 2010; Wang *et al.*, 2012; Arat *et al.*, 2015). Moreover, the thermal efficiency was reported to be higher for port injection than in-cylinder method at all equivalence ratios (Yi *et al.*, 1995) and increase with increase in concentration of hydrogen for dual fuel mode (Varde, 1983). In this type of hydrogen application, hydrogen contributes an insignificant amount of direct kinetic energy toward moving the engine's pistons. In other words, hydrogen delivers its primary benefit by enriching the fuel, not by acting as the primary energy source.

The other advantage of using hydrogen gas as fuel supplement in internal combustion is the improvement in engine emission characteristics of both compressed and spark ignition engine. The reduction in engine emission due to hydrogen addition is found to vary from 7%-20% for CO and 5-9.5% for HC (Yilmaz *et al.*, 2010; EL-Kassaby *et al.*, 2016). The emission characteristics of CO and HC are reported to depend upon the load of the engine. At constant 1500 rpm for a four cylinder CI stand-alone engine, reduction in CO and HC are 9.81% and 54.55% at 19 kW load with 31.75 L/min direct injection induction of $H_2/ O_2$ and is lower, 9.19% for CO and 49.48% for HC at higher 28 kW load at 30.6 L/min induction of $H_2/ O_2$ (Bari, 2010). The emissions level of CO is further reported to decrease from 6 ppm to 3 ppm at engine speed between 2133-2745 rpm and increased to a maximum level of 22 ppm between 2745-3500 rpm and then decreases to zero for eight cylinder SI engine (Kilicarslan *et al.*, 2017). However for NOx, while a

reduction of 15%-50% on the average has been reported (Musmar, 2011; Tamer, 2018; EL-Kassaby *et al.*, 2016), other studies observed increased emission level of the gas (Bari, 2010; Birtas, 2011; Anh *et al.*, 2013). The $NO_x$ emissions depends on the engine load, engine compression ratio, hydrogen enrichment level and the lean burn condition because all these factors cause increase in temperature which leads to the formation of NOx (Varde *et al.*, 1983; Yilmaz *et al.*, 2010).

At the same time, there are some contrasting reports on the use of hydrogen as fuel additives. The effect of hydrogen addition on HC and CO emissions does not always result in their reduction. Saravanan and Nagarajan found that the addition of hydrogen increased HC emissions from 28 ppm when running on diesel only to 31 ppm at 25% of full load while at 75% of full load the emissions with and without hydrogen were similar (Saravanan *et al.*, 2007). Samuel and McCormick also reported that at 1500 rpm and 5.3 bar break mean effective pressure engine load of CI engine, the emissions of CO first decreases upto 2.2 LPM of hydrogen and then increases with increase in hydrogen content due to decrease in duration of combustion and rise in pressure. The smoke level is also found to increase with increase in supply of hydrogen (Samuel, 2010). When experimenting with lean mixtures, Ji and Wang found that the addition of hydrogen gas resulted in increased CO emissions close to stoichiometric lean mixtures. This was attributed to the faster reaction rate of hydrogen with oxygen in air compared to petrol, resulting in oxygen depleted zones within the mixture and also because of the longer post-combustion period (resulting from the faster combustion) that cooled the in-cylinder gases before being exhausted thereby reducing the rate of CO oxidization into $CO_2$. One

disadvantage of hydrogen enrich fuel is the increase in the emissions of $NO_x$ at high temperature.

In the above method of fuel enrichment, hydrogen gas is obtained either from bottled compressed hydrogen gas or through water electrolysis. Due to the problems associated with compressed hydrogen gas such as cost, storage, availability and danger, the other method, water electrolysis has been considered to be the most convenient technique for hydrogen gas generation in fuel enrichment application. Water electrolysis although simple have serious drawback in term of efficiency. The main factor in the decline of efficiency is the electrical resistance associated with bubbles formation at the electrodes, overpotential, ionic transfer and electrical circuit. One way to improve the efficiency depends on the electrolyzer design and in this regard common-ducted multiple plate configurations with alkaline electrolytic solution is the design used in most studies. The gas obtained from such electrolyzer is not pure hydrogen but a mixture of hydrogen and oxygen in stoichiometric ratio called Brown's gas or hydroxy gas (HHO). As far as the electrolytic solution is concerned alkaline electrolysis is preferred over acidic due to the fact that the latter have greater tendency to cause corrosion of metals (Kreuter, 1998). The advantages of employing water electrolysis are:

    i)        HHO gas, apart from retaining all the properties of hydrogen gas, its additional oxygen content helps in combustion of the fuel much more efficiently

    ii)       The simplicity and robustness of the electrolyzer design makes it convenient for on-board vehicle application

iii)      Possibility of hydrogen gas production at the point of use eliminating the danger involve in storing the gas

Moreover, there are some observations that show that the combustion of Brown's gas differs from normal hydrogen-oxygen mixture. The difference includes the ability to melt metals with very high melting point but have a relatively cool flame. The flame temperature of hydroxy gas varies from 150-9000 $°C$ depending on the nature of the material to which it is applied. Moreover, the specific weight of HHO gas is reported to be 12.3 g/mol while the specific weight of stoichiometric mixture of $H_2$ and $O_2$ is 11.3 g/mol indicating an anomaly, suggesting the presence of new molecules while some reported the stoichiometric mixture to be 12 g/mol, the (Santilli, 2006; Calo, 2007). The higher weight of HHO is considered to be due to presence of water vapour by Calo JM. However, the work published by Santilli is doubtful because the maximum temperature that hydrogen gas flame can reached is $2800°C$, therefore   HHO flame temperature of $9000°C$ as reported by Santilli is not thermodynamically possible. Moreover, hydrogen and oxygen gases, being homonuclear molecules are inactive in IR spectroscopy and hence will not show IR absorption in the spectrum. Therefore, the IR spectra reported by Santilli is not the IR spectra of either Oxygen or Hydrogen. Since the reference spectra are not the spectra of either $O_2$ or $H_2$, the suggested new compound is also doubtful. Thus, in the present work the water electrolysis product is assumed to be stoichiometric mixture of $H_2$ and $O_2$ mix with water vapour.

There is a difference between the effects of application of compressed hydrogen and application of Brown's Gas obtained directly from a common-ducted electrolysis unit for use as a fuel supplement in internal combustion engines. The

engine performance such as brake power, torque and specific fuel consumption is higher with the use HHO as compared to pure hydrogen (Baltacioglu *et al.*, 2016). The high flame temperature and additional oxygen content in HHO helps to burn the fuel much more efficiently than hydrogen. Hence, the emission level of HC, CO and $CO_2$ are much lesser when using HHO as compared to pure hydrogen gas.

      The main objective behind the used of hydrogen in all these research is to develop ways to reduce the fuel consumption and at the same time, reduces the amount of harmful emitted pollutant gases. However, all the earlier published works that had been highlighted above on the application HHO gas fuel supplement are based on experiments conducted in engine test rigs and stationery engine. As a result, the published data may not be directly applicable to a vehicle system as a whole due to many competing factors that would try to reduce the beneficial effects of hydrogen addition. Moreover, most of the existing works reports the benefits of using HHO gas without a clear picture on whether the power consumption and losses in the battery, vehicles alternator and electrolyser have been taken into account. Different analysis based on feasibility in terms of applicability and power requirements on road transport system only will show the real effects on whether hydroxy gas as fuel supplement proves to be a potential candidate for fuel economy and reduction in the harmful emissions. Thus, this research work is born to determine whether hydroxy gas as fuel supplement is applicable on actual road transport system in providing a means to reduce the global fuel consumption rate and reduce greenhouse effect caused by petrol based transport sector creating cleaner, better environment for the human race.

# CHAPTER 2
# MATERIALS
# &
# METHODOLOGY

## 2. MATERIALS AND METHODOLOGY

This section describes the different theory, equipment's and techniques used to perform the different experiments in this work. This chapter is broadly classified into three main sections: (i) Generation of HHO gas (ii) Test Vehicle and (iii) Fuel Economy measurement (Mileage Measurement)

### 2.1 Generation of Brown's gas (Hydroxy gas/HHO gas)

The electrolysis process, the nature of electrolytes, the type of electrolyzer, HHO production rate measurements and safety precautions are some of the things to be considered during the generation of HHO gas that are given in this section. The methods of on-board fitment of the HHO electrolyzer on Maruti 800 and methods for controlling the rate of production of HHO gas are also describe in detailed.

### 2.1.1 Theory of Electrolysis

Electrolysis of water is the splitting of water ($H_2O$) molecule into oxygen ($O_2$) and hydrogen gas ($H_2$) by passing an electrical current through it. The basic principle of electrolysis is governed by the two Faraday's Law of electrolysis. These laws relate the amount of liberated mass at an electrode to the quantity of electricity passing through the electrode. The two Faraday's laws of electrolysis are

*Faraday's 1st Law of Electrolysis*: The mass of a substance produced at an electrode during electrolysis is directly proportional to the number of electrons (the quantity of electricity) transferred at that electrode.

*Faraday's 2nd Law of Electrolysis*: The number of Faradays of electric charge required to discharge one mole of substance at an electrode is equal to the number of

excess elementary charges on that ion. So, Faraday's laws are summarized by Eqn 2.1

$$m = QM/zF \tag{2.1}$$

where m is the mass of the substance produced at the electrode, Q is the total electric charge passed through the solution, z is the valence number of ions of the substance (electrons transferred per ion), $F = 96\ 485$ C mol$^{-1}$ is the Faraday constant, and M is the molar mass of the substance. One faraday of charge is the magnitude of the charge of one mole of electrons. The total charge Q is the integral electric current I (t) over time t and can be described as

$$Q = \int_0^{t_{tot}} I(t)dt \quad \text{or} \quad Q = \int_{t_1}^{t_2} I(t)dt \tag{2.2}$$

where $t_{tot}$ is the total amount of time of the electrolysis. In the simple case of constant current electrolysis, the integral evaluates to

$$Q = I \cdot t_{tot} \quad \text{or} \quad Q = I \cdot (t_2 - t_1) \tag{2.3}$$

and leads to Eqn 2.4

$$n = \frac{I \cdot t_{tot}}{zF} \tag{2.4}$$

where n = (number of moles) produced: n = m/M.

The electrical conductivity of pure water is very less, about one millionth that of seawater, thus, electrolyte such as an acid or a base is added to pure water to increase up its electrical conductivity. The main advantage of alkaline electrolysis over other water electrolysis is because alkaline electrolyzers can be made of abundant and inexpensive materials such as simple iron or nickel steel electrodes, its simplicity and environmental friendly for producing high purity hydrogen (Cardona *et al.*, 2016). According to a number of studies, water electrolysis is affected by a

number of factors such as electrolyte concentration, temperature, current density and voltage, it is therefore paramount important to understand the operational characteristics of the overall electrolytic system (Zeng, 2010; Bockris *et al.*, 2004; Isao, 2009)

**2.1.2 Alkaline Electrolysis**

Alkaline electrolysis is based on the principle that under the influence of an electric field water molecule undergoes oxidation and reduction at the anode and cathode electrode forming oxygen and hydrogen gas respectively after recombination of atomic state. The most basic water electrolysis set up is shown in **Figure 2.1** and the reaction involved is given below.

$$\text{(Cathode)} \quad 2H_2O + 2e^- \quad \rightarrow 2OH^- + H_2 \uparrow \tag{2.5}$$

$$\text{(Anode)} \quad 2OH^- \quad \rightarrow H_2O + 2e^- + \tfrac{1}{2}O_2 \uparrow \tag{2.6}$$

$$\text{(Total)} \quad 2H_2O \quad \rightarrow H_2 + \tfrac{1}{2}O_2 + H_2O \tag{2.7}$$
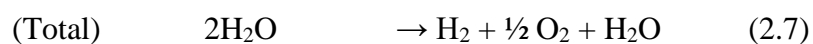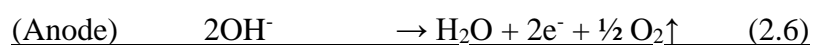
At the cathode two molecules of water undergo reduction producing one molecule of hydrogen and two hydroxyl ions as given in Eqn 2.5. Hydrogen escapes from the surface of the cathode in a gaseous form. The hydroxyl ions move to the anode under the influence of the electrical field, where they are oxidized to l/2 molecule of oxygen and one molecule of water (Eqn 2.6). The oxygen recombines at the surface of the anode and escapes as oxygen gas (Kreuter, 1998; Isao, 2009).

**2.1.3 Thermodynamic aspects of Electrolysis**

According to Faraday's laws of electrolysis, the amount of gas produced is directly proportional to the current flowing through the electric circuit which in turn is determined by the cell potential. The minimum workdone required to start electrolysis process can be derived from thermodynamic treatment of the problem.

The minimum cell potential $E^o_{cell}$ or open circuit potential is the amount of the potential difference, under equilibrium cell current, between the two half cells in an electrochemical cell that enables electrons to flow from one electrode to the other for the production of hydrogen gas. It is given by

$$E^o_{cell} = E_{anode} - E_{cathode} \qquad (2.8)$$

The equilibrium cell potential is also referred to as the electromotive force in battery and counter electromotive force in electrolyzer. The minimum reversible workdone ($w_{electrical}$) in an electrochemical cell for electrolysis can be mathematically formulated as

$$w_{electrical} = charge \; x \; minimum \; potential = -QE^o_{cell} \qquad (2.9)$$

From Faraday laws,

$$Electric \; charge, Q \; = \; nF \qquad (2.10)$$

$$w_{electrical} = -nFE^o_{cell} \qquad (2.11)$$

where n = number of moles of electrons transferred or that flow through circuit,

F = 96,483 Cmol$^{-1}$ is Faraday's constant

According to the first law of thermodynamics, the change in internal energy of a system is equal to heat absorbed by the system and the workdone by the system

$$\Delta U \; = q + w \qquad (2.12)$$

The work done $w$ may be reversible as well as non-reversible. Therefore Eqn 2.12 can be written as

$$\Delta U = q + w_{reversible} + w_{non-reversible} \qquad (2.13)$$

At constant pressure, the reversible workdone is given by $w_{reversible} = -P\Delta V$ , thus

$$q = \; \Delta U + \; P\Delta V - w_{non-reversible}$$

But enthalpy, $H = \; U \; + \; PV \implies \Delta H \; = \; \Delta U \; + \; P \; \Delta V$, therefore

$$q = \Delta H - w_{non-reversible} \qquad\qquad (2.14)$$

For a reversible change taking place at constant temperature, change in entropy $\Delta S$

$$\Delta S = q_{rev} / T$$

$$\text{Or } q_{rev} = T\Delta S \qquad\qquad (2.15)$$

Using Eqn 2.14 in 2.15,

$$T\Delta S = \Delta H - w_{non-reversible}$$

$$\Delta H - T\Delta S = w_{non-reversible} \qquad\qquad (2.16)$$

where q= heat absorbed by the system, T= Temperature, U= internal energy, p = pressure and V= Volume

The Gibb's free energy is a thermodynamic potential that can be used to calculate the maximum of reversible work that may be performed by a thermodynamic system at a constant temperature and pressure and is given by

$$G = H - TS$$

Thus, Gibb's free energy change is

$$\Delta G = \Delta H - T\Delta S \qquad\qquad (2.17)$$

Substituting Eqn 2.16 in 2.17,

$$\Delta G = w_{non-reversible} \qquad\qquad (2.18)$$

Since the non-reversible $w_{non-reversible}$ workdone is the same as the work done on a reversible electrochemical cell $w_{electrical}$

$$\Delta G = -nFE^o_{cell} \qquad\qquad (2.19)$$

Thus, the minimum amount of cell potential $E^o$ required for electrolysis at constant temperature and pressure is given by

$$E^o_{cell} = -\frac{\Delta G}{nF} \qquad\qquad (2.20)$$

In an open cell, for electrolysis of water $\Delta G = \Delta H - T\Delta S = 237.2$ kJ/mol at 1 bar, 25ºC and two electrodes are needed for electrode reaction, therefore, the reversible cell potential is given by

$$E^o_{cell} = -\frac{\Delta G}{nF} = \frac{237.2}{2\times 96493}10^3 = 1.229V \tag{2.21}$$

Hence the minimum cell voltage or the reversible potential required for electrolysis in electrolytic cell is $E^o_{cell} = 1.23V$ (Zeng, 2010). Thus Faraday efficiency of electrolysis will be expressed as

$$Farday\ efficiency, \varepsilon_f = \frac{1.23V}{E_{cell}} \tag{2.22}$$

However, the actual cell voltage for the electrolysis process to start is higher than reversible potential because of overpotential- overpotentials due to activation energy, ionic transfers and electrical circuit resistance. Due to these overpotentials, the minimum cell voltage required for practical electrolysis is estimated to be 1.48 V called Thermoneutral Voltage (Zeng, 2010). Thus, the electrolysis efficiency is determined by the thermal efficiency and is defined as the ratio of the change in enthalpy to the sum of Gibb's free energy change and energy losses (at standard conditions of 1 bar at 25ºC).

As shown in **Figure 2.2**, below the thermoneutral voltage, the electrolysis process is endothermic, that is, heat generated by overpotential is absorbed back by the reaction until total cell voltage exceeds the thermoneutral voltage of 1.48 V. Since in water electrolysis the current efficiency is very high, almost reaching 100%, the electrical the energy efficiency of the alkaline water electrolysis can be approximated by the relation (Isao, 2009)

$$Thermal\ efficiency = \frac{Thermoneutral\ Voltage}{Cell\ Voltage} = \frac{1.48\ V}{Cell\ Voltage} \qquad (2.23)$$

Thus, thermoneutral voltage can be used as a reference for estimating efficiency of practical electrolysis

## 2.2 Electrolyzer

Electrolyzers are of two types depending on the cell configuration namely monopolar and bipolar electrolyzer cells (Bockris *et al.*, 1981). In monopolar cells, DC power of opposite polarity is supply to each of the electrodes that are arranged in alternate position as given in **Figure 2.3 (a)**. As a result, each electrode acts as individual cells in parallel combination of monopolar arrangement. Hydrogen and Oxygen evolution reaction takes place on both sides of each electrode. Each cell has the same operating voltage and the total voltage of the entire electrolysis cell is equal to the sum of the voltage of each individual cell.

In bipolar cells, the DC power supply is connected to only the outermost electrodes as shown in **Figure 2.3 (b)**. The electrodes stacked between the outermost electrodes are activated by the electric field making each electrode positive on one side and negative on the other side. Hydrogen and Oxygen formation occurs on the opposite side of same electrode simultaneously. Adjacent electrodes are electrically linked in series with each other forming a unit cell. The sum of the voltage of each unit cell is equal to the total voltage of the whole unit. In industrial process, the parallel cell connection in monopolar configuration leads to lower cell potential of 2.2 V as compared to series connection in bipolar arrangement which has cell potential of 2.2 × (n-1) V, where n is the number of electrodes (Bockris *et al.*, 1981). An advantage of the bipolar cells stack design is that the electrodes are placed closed

to each other reducing the losses due to the internal ohmic resistance of the electrolyte and bubble formation.

Among the bipolar configuration, again there are two types of electrolyzer design-wet cells and dry cells. The wet cells have high stability, have high gas production rate and are easy to maintain as compare to dry cells. However, they have high tendency to consume more power, higher induction of heat through the cells leading to formation of water vapour and corrosion of the anodes (Egan *et al.*, 2013; Ismail *et al.,* 2018). It is this context that leads to the development of the dry cell. The dry cell is design to overcome all the drawbacks of the wet cell, at the same time retaining all the advantages of the wet cell. It is different from wet cell in terms of electrolyte vessel and position of the electrode plates. The compact design of the dry cell leads to higher volumetric concentration of electrolytes thus demanding less current, reduction of the anode corrosion and ease of installation on on-board vehicle (Egan *et al.*, 2013; Ismail *et al.,*2018). A dry cell design produces more gas than other electrolyzers because almost all the entire area of the electrodes are used for the electrolysis process and all the electrolyte solution are being used and charged with current.

**Figure 2.4** shows the HHO Dry Cell electrolyzer unit which was obtained directly from HHO2U, USA. The design was based on common-ducted dry cell concept. There are 3.5 x 3.5 18 gauge 1 mm thick 11 plates made of 316 L stainless steel, and arranged in series having a total of 10 separate cell chambers. Each electrode is separated from the others by about 1.5 mm using 7 cm diameter O ring. The O Rings are made of Buana 70 Nitrile heat resistant to 260 degrees. Three holes in vertical direction are provided in each plate for better circulation of the solution

and gas. These electrodes are finally enclosed between two Acrylic end caps attached with two hose barbs for inlet of solution and outlet of gas. The Acrylic end caps are 100 mm X 100 mm X 12 mm thick rated at 145 degrees C. The 2 hose barbs are 1/4. The attachment bracket angles are aluminium 2 X 6 mm SS wing nuts for easy connection to the power source. The arrangement of the plates and the holes configuration enabled the dry cell design to produce maximum amount of HHO gas with the least amperage draw.

Electrically, the cell structure is a series-parallel combination of electrodes in the form -nnnn+nnnn-, where'+', '-'and 'n' indicate the positive, negative and neutral plates respectively as shown in **Figure 2.5**. The neutral plates caused the dry cell to evenly distribute the voltage between the plates causing the cell to run at lower temperature. Knowing the power efficiency of the electrolyzer and operation at its most efficient point is an important parameter for the feasibility of application of HHO dry cell generator on-board the vehicle understudy.

**2.3 Power Supply Controller and Measurement**

**2.3.1 Measurement of Current**

For current measurement ordinary multimeter cannot be used as they limit the current according to their capacity. Therefore for current measurement shunt resistor, given in **Figure 2.6**, rated for 100 A at 75 mV made of low temperature coefficient material called manganin is used and is placed in series with the electrolyzer. Manganin, because of its small temperature dependence, high specific electrical resistivity and small temperature coefficient is considered to be a highly reliable means of current measurement.

When the current flows through the shunt resistor, a voltage drop is generated across it which is proportional to the current flowing through it. This voltage drop is measured with a multimeter connected in parallel with the shunt resistor as shown in **Figure 2.7**. This voltage drop is then used for calculating the corresponding value of current using Ohm's law.

$$I = \frac{V}{R} \qquad (2.24)$$

where I is measured in Ampere is measured in volts and R in Ohms.

### 2.3.2 Power Supply Controller

Pulse Width Modulator (PWM) was used to regulate power supplied to the electrolyzer. **Figure 2.8** shows the Pulse Width Modulator used in this work that was purchased directly. It has the following specifications

- Working voltage: DC10 V- DC 50 V.

- Maximum output current: 40 A.

- Control Motor Power: 0.01-2000 W.

- Working voltage 12 V: 12 V*40 A=480 W (max).

- PWM Frequency: 7.5 kHz.

PWM provides variable pulse width with fixed frequency. The duty cycle of the pulse width modulator is adjusted with the help of potentiometer. First, the potentiometer position is calibrated in terms of duty cycle using CRO. Duty cycle is the amount of time the signal is in a high (on) state as a percentage of the total time of it takes to complete one cycle. It is given by the relation

$$Duty\ Cycle = \frac{Pulse\ width}{Total\ Period\ of\ the\ Waveform} \times 100\% \qquad (2.25)$$

Then based on the duty cycle, the potentiometer position was marked in interval of 10 within a range of 0-100%. The duty cycle can be varied from 0- 100%.

## 2.4 Measurement of Temperature

An infrared thermometer MT8530 was used to measure temperature, it has ratings of (-50 ~ 530) $^{o}$C, accuracy of $\pm$ 2% (**Figure 2.9**). The distance to spot (DS) ratio is maintained as per instruction at 12:1. This DS ratio enables us to cover one side of the electrolyzer for measurement.

## 2.5 Measurement of HHO Gas Production Rate

The experimental set-up for producing hydrogen gas is shown in **Figure 2.10**. The alkaline solution is prepared by dissolving potassium hydroxide (KOH) of analytical reagent grade in distilled water. When potassium hydroxide is dissolved in distilled water, heat is liberated indicating dissolution of KOH is exothermic. In this work, the concentration of electrolyte is measured in molarity and it is in the range 1 M to 2 M. One molarity is defined as

$$Molarity = moles\ of\ solute/\ Liters\ of\ solution$$

$$\text{Or } Molarity\ (M) = \frac{grams\ of\ solute\ \times 1000}{molar\ mass\ of\ solute\ \times molar\ mass\ of\ solvent} \qquad (2.26)$$

The electrolytic solution was cool down to room temperature before used. Power supply for electrolysis is directly obtained from the battery of Maruti 800 (Type II), which is charged to its full capacity before each experiment. The power supplied from the alternator is fed to the pulse width modulator before feeding to the electrolyzer. This arrangement was made to regulate the amount of power supply and hence the rate of production of HHO gas using the PWM potentiometer. An analog ammeter which used 10A fused was fitted at the power supply line of HHO generator.

The current flowing to the electrolyzer unit was measured using both the ammeter as well as by the voltage drop across the shunt resistor using Scientech 4011 digital multimeter. An exhaust fan was incorporated at the PWM assembly to cool down the excess heat generated by the electrical circuit. The temperature of the solution and the electrolytic plates during electrolysis was measured simultaneously using both MT8530 Infrared Thermometer and alcohol thermometer. The voltage of the electrolyzer cell was measured with a Scientech multimeter 4011.

The electrolytic solution is stored in a separate reservoir tank from which it is supplied to the electrolyzer by gravity through the feed line. The electrolytic solution that enters the electrolyzer is subjected to current and undergoes electrolysis. **Figure 2.11** shows a complete circuit diagram of current supply to the HHO Dry Cell. The current supplied to the electrolyzer varied depending on the duty cycle of the PWM. The length of the duty cycle is controlled through the potentiometer of the PWM. The electrolytic solution after electrolysis goes back to the reservoir tank through the return line. The return line is always occupied by column of the solution creating pressure on the electrolysis process together with the gas inside the tank. This process repeats over and again, undergoes electrolysis which results in the accumulation of HHO gas at the reservoir tank above the electrolytic solution. The HHO gas is taken out from the reservoir tank using an acrylic pipe. The pipe is fitted at the top of the tank and is fed to the Bubbler via a flashback arrestor valve as shown in **Figure 2.12**. It is important to note that the HHO gas produced is always accompanied by water vapour. The bubbler is a transparent plastic bottle partially filled with water. The water vapour associated with the HHO gas is condensed in the bubbler. This helps in improving the purity of the HHO gas concentration. The HHO

gas with high purity is then taken out using an acrylic pipe fitted at the top of the bubbler and is finally supplied to the point of application. The HHO gas production rate was measured by downward displacement of water under atmospheric pressure. Each observation was repeated at least 3 times for 30 sec and the uncertainties in measurements are $1^o$ C in temperature and $\pm 10\%$ in the gas flow rate. The total duration of electrolysis for each series of experiment is about 2.5 hrs.

## 2.6 Safety Measures

HHO gas is highly combustible in nature which usually results in backfiring at the air intake and/or exhaust system. The backfiring limits the performance of an internal combustion engine and proves hazardous for hydrogen fuel enhancement system. Due to such reason, backfiring is a crucial factor to be considered when hydroxy gas is used as fuel additive. Rudolph Erren devised a method called Errenizing to overcome the problem of backflash. In this method, slightly pressurized hydrogen is injected into air or oxygen inside the combustion chamber (Hoffman P., 2001). Lower explosive limit (LEL) (Antunes *et al.*, 2009), flame arrestor, flame trap, bubbler, water trap, water arrester or valves for pressure regulator are also generally installed on hydrogen fuel enhancement system to prevent flashback/backfire (Antunes *et al.*, 2009; Suryawanshi, 2011; Karagöz *et al*.,2015; Ganesh *et al*, 2008). In the present work, a bubbler was used along with a flashback arrestor in the gas output line. This serves as safety precaution against backfire and explosion of gas.

## 2.7 On-Board Fitment of HHO generator

The HHO generator is placed at the floor of front passenger side of the test vehicle. Hydrogen rich gas or Brown's gas obtained from the electrolyzer is applied through a plastic pipe to the engine by port injection to the engine air intake manifold.

This method does not require any major modification to the engine hardware. The power supply for electrolyzer is obtained from a 12 V lead accumulator, which is placed at the back compartment of Maruti 800.

**2.8 Technical Specification of Maruti 800 (Type II)**

Maruti Udyog 800 (Type II) is a four stroke, 3-cylinder internal combustion engine operating on gasoline fuel and has fuel tank capacity of 28 L. The piston displacement of Maruti 800 is 796 cm$^3$ and a compression ratio of 9.2:1. A battery of 12 V, 24 AH with an alternator rating of 35 A was used in the test vehicle. Most of the light system in this engine has a voltage handling capacity of 12 V with a 60/55 W headlight, 21 W turn signal light and side turn signal light of 5 W. The mileage specified by the manufacturer is 13.1 km/L in city and 16.1 km/L on highway with an average mileage of 15.5 km/hr.

The air-fuel ratio 14.7:1 of the test vehicle Maruti 800 is maintained by the Engine control Unit (ECU) based on the data given by the sensors such as vehicle speed sensor, oxygen (lambda) level sensor and engine coolant temperature sensor by way of electrical signals. Depending on the information supplied by the different sensors, the ECU controls the various operating parameters such as the fuel injection timing and the RPM of the engine by delivering the correct amount of fuel required to maintaining the ideal air-fuel mixture.

Under idle condition, the air-fuel ratio is maintained by a narrow band lambda (oxygen) sensor located upstream of the catalytic converter in the car exhaust system. The sensor provides voltage signal variations within $\pm 1$ V. This sensor determines the rich and lean mixtures by comparing the amount of oxygen between the exhaust gas and the atmosphere. It then relays information to the ECU in the

form of voltage and the ECU finally adjusts the amount of fuel accordingly. Hence, the lambda sensor not only helps in maintaining the air-fuel ratio, but also controls the level of emission by the test vehicle.

The exhaust emission level of Maruti 800 is also controlled by catalytic converter through oxidation-reduction mechanism. The catalytic converter attached to the exhaust pipe is a heat–resistant honeycomb porous material that is coated with reduction catalyst (platinum or rhodium) and oxidation catalyst (platinum or palladium). The reduction catalyst breaks oxides of nitrogen into nitrogen and oxygen atoms. The oxidation catalyst oxidized carbon monoxide (CO) to carbon dioxide and unburned hydrocarbons to carbon dioxide and water.

The power required for up and down movement of the piston in the test vehicle is obtained by ignition of the petrol. In an internal combustion engine, the combustion of fuel in the cylinder creates a pressure that exerts a downward force on the piston. The force is transmitted from the piston to the crankshaft through the connecting rod which is attached to the crankshaft at a certain distance from the center of the shaft. The piston starts moving up and down in rotational motion. The motion of piston is measured in terms of Rotations Per Minute (RPM). Thus, engine RPM measures the rotational speed of the crankshaft of the engine and determines the speed of the engine. The number of 360 degrees rotation of the crankshaft within one minute is termed as Revolutions Per Minute (RPM). An external Yeeco Digital LCD Hour Meter Gauge Tachometer RPM Meter fitted on the dashboard is used for measuring the RPM of the vehicle. The burning of fuel in the combustion chamber increases on pressing the accelerator which provides more power to the piston.

Consequently the engine RPM increases. However, maximum RPM does not necessarily mean maximum power of the engine. The manufacturer specification of the vehicle determines the RPM at which the maximum power can be reached. For the test vehicle, the maximum power is 37 BHP and maximum torque is 2500 rpm.

**2.9 Measurement of Fuel Economy**

**2.9.1 Calibration of Fuel Sending Unit**

The fuel sending unit is a device for measuring the amount of fuel in the fuel tank of automobiles. It consists of a float connected to a metal rod which is attached to a variable resistor. The variable resistor acts as a rheostat and contains a strip of resistive material grounded on one side. This resistor sends an electronic signal to the fuel display. A simple example of fuel level indicator system and its electrical connection used in commercial vehicle is given in **Figure 2.13**. The electronic signal comes from the car battery via a small coil made of copper wire. The resistance of the variable resistor is at its minimum value when the fuel tank is full, and increases as the float drops. As the fuel is consumed, the rod slides along the resistor which gradually increases the resistance. However, due to irregular shape in the design of the fuel tank, the fuel level might not change even when the fuel is consumed. This makes it impossible to observe accurate readings while studying the specific fuel consumption (SFC) rate.

**2.9.2 Mileage Measurement**

Mileage is the distance travelled by a motor vehicle per unit amount of fuel consumed and it is a direct indicator of the fuel economy or fuel efficiency of the vehicular system. To investigate the effect of fuel economy, the parameter mileage is

used. To measure mileage correctly, determination of the amount of fuel consumed is needed. Therefore a method is device where the fuel sender unit (FSU) is calibrated with respect to the amount of fuel present in the fuel tank. To calibrate the fuel sender unit resistance, the vehicle is first positioned horizontally and all the fuel is piped out from the fuel tank. Next a digital multimeter in resistance mode is connected to the FSU line and the resistance reading (in ohm) is noted. Then the fuel is added back in step of 1 L each and the change in resistance is noted. This step is continued till the tanky is full. Next the amount of fuel added to the resistance is plotted and the slope of the graph is used for determining the amount of fuel consumed and hence the mileage of the test vehicle.

## 2.10 Measurement of Vehicle Emissions

The tail pipe emissions of the vehicle understudy is studied using gas analyzer. **Figure 2.14** shows the i3 Sys Gas Analyzer EPM1601 which is in compliance with BAR-97, OIML class 0 and ISO3930 international standards, Indian Standard CMVR/TAP-115/116 issued by Ministry of Road Transport & Highways. It is specifically design to measure the rate of emission of carbon dioxide, hydrocarbons and carbon monoxide through the principle of Non-Dispersive Infra-Red, and oxides of nitrogen, oxygen and oxides of Sulphur by electrochemical principle. The technical specifications of EPM1601 are given in **Table 2.1.** The EPM1601 required warm up time of two minutes after which it performs self-diagnostic test like leak check and zero error. The vehicle settings are done to select the type of vehicle, petrol and number of cylinder used. After the vehicle settings, self-diagnostic hydrocarbons residue check is done and the engine of the vehicle is turn on and then accelerated for 20 seconds. The engine is then returned to idle

position/neutral position and the sampling probe of length 7cm of the EPM1601 gas analyzer is inserted to the tail pipe of the vehicle under study. The exhaust emission characteristic is observed and recorded either through display screen of the gas analyzer or the laptop that is interfaced with the gas analyzer using XCTU software.

XCTU is used for reading the data from the analysis through a computer. It a free multi-platform application designed to enable developers to interact with Digital Radio Frequency modules through a simple-to-use graphical interface. It can manage and configure multiple devices, even remotely (over-the-air) connected devices. The firmware process seamlessly restores module settings, automatically handling mode and baud rate changes. The XCTU save the console sessions and load them in a different PC while running it. The Serial console tool of the XCTU allows direct communication between the laptop and the gas analyzer (i3sys User Manual, 2012).

**List of Figures**
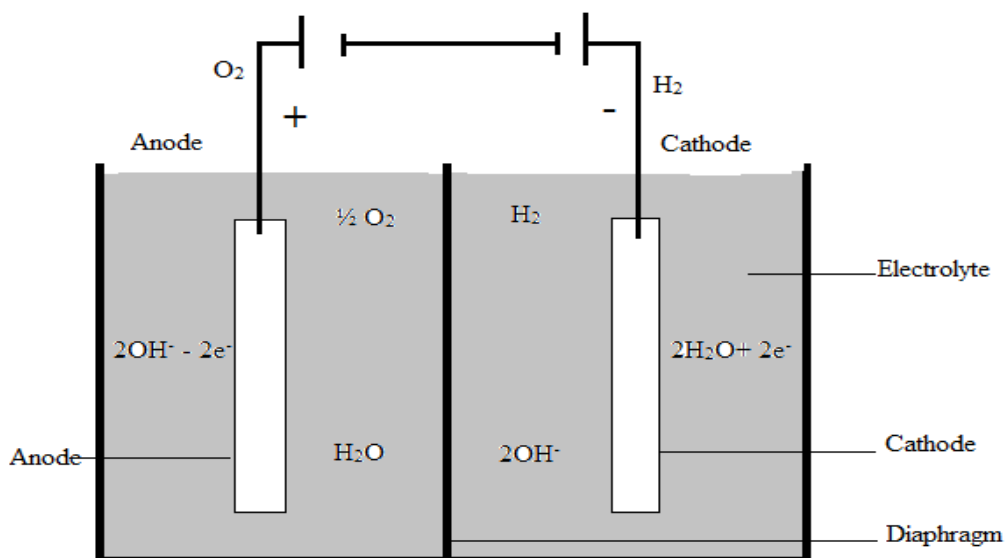


**Figure 2.1:** Principle of alkaline electrolysis (Kreuter, 1998)
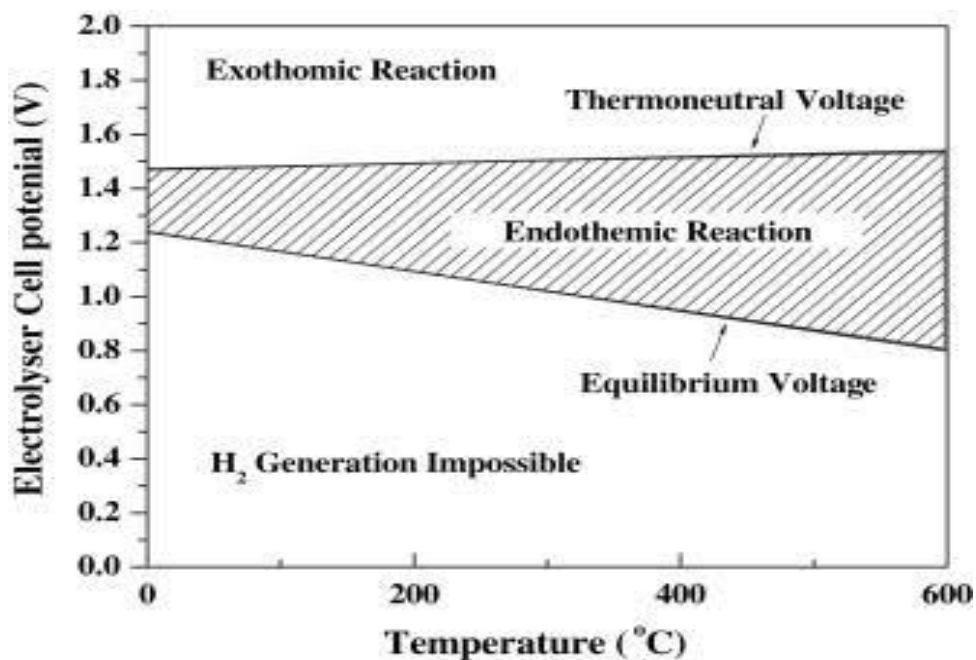


**Figure 2.2:** Cell Potential for hydrogen production by water electrolysis as function

of   temperature (Zeng, 2010)
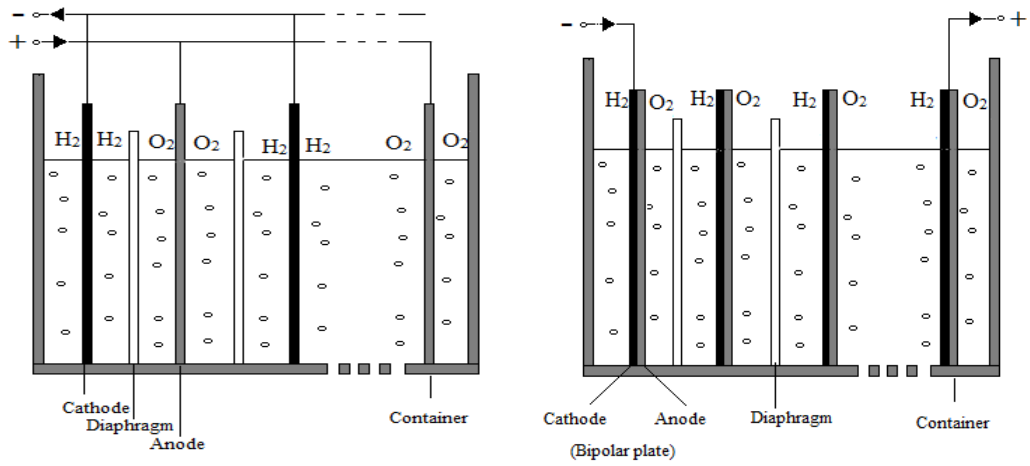
**Figure 2.3 (a)**: Monopolar Electrolyzer    **Figure 2.3 (b)**: Bipolar Electrolyzer
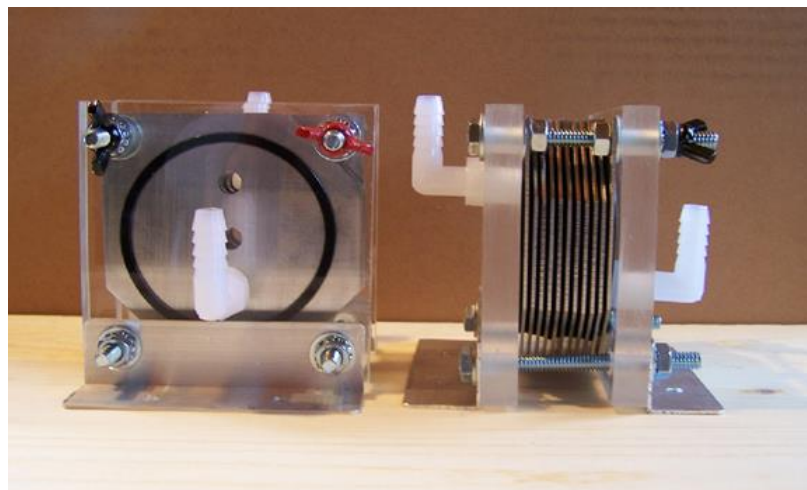


**Figure 2.4:** HHO Dry Cell Electrolyzer
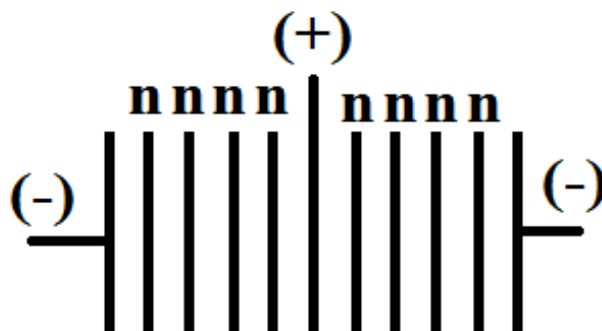


**Figure 2.5:**  Electrical Structure of 11 plates HHO dry cell

**Figure 2.6:** Shunt resistor
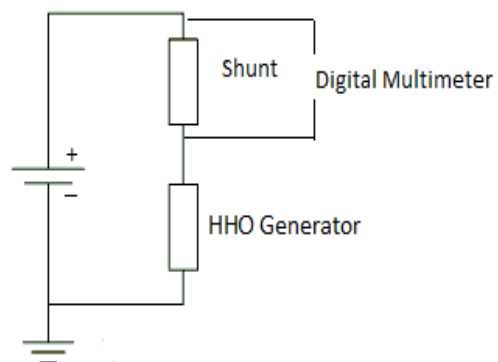


**Figure 2.7:** Circuit Diagram of Shunt Resistor connection to load



**Figure 2.8:** Pulse Width Modulator

**Figure 2.9:** MT8530 Infrared Thermometer



**Figure 2.10:** Experimental set-up for production of HHO gas
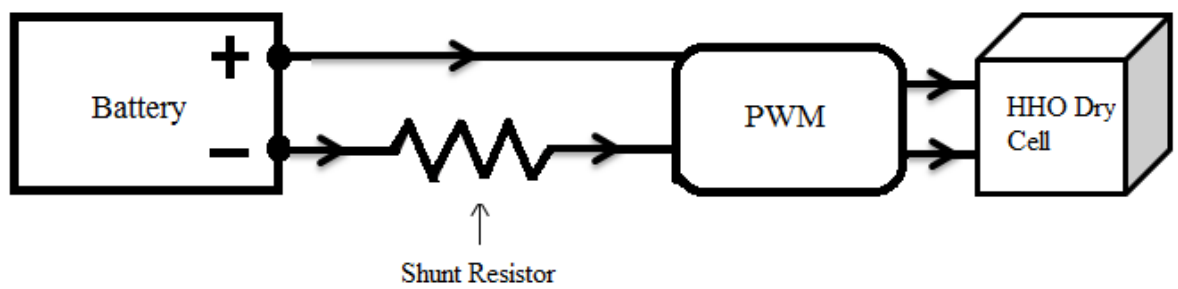


**Figure 2.11:** Circuit Diagram of current supply to HHO Dry Cell
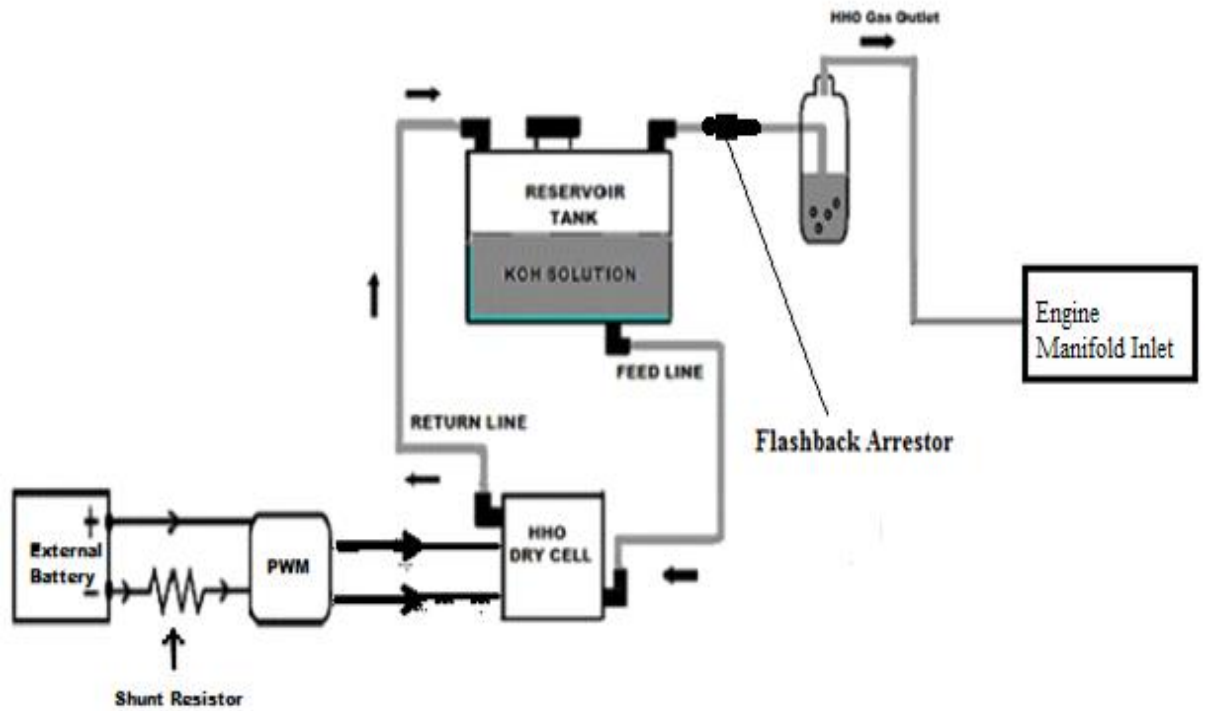
**Figure 2.12:** Block Diagram for Measurement of production of HHO gas
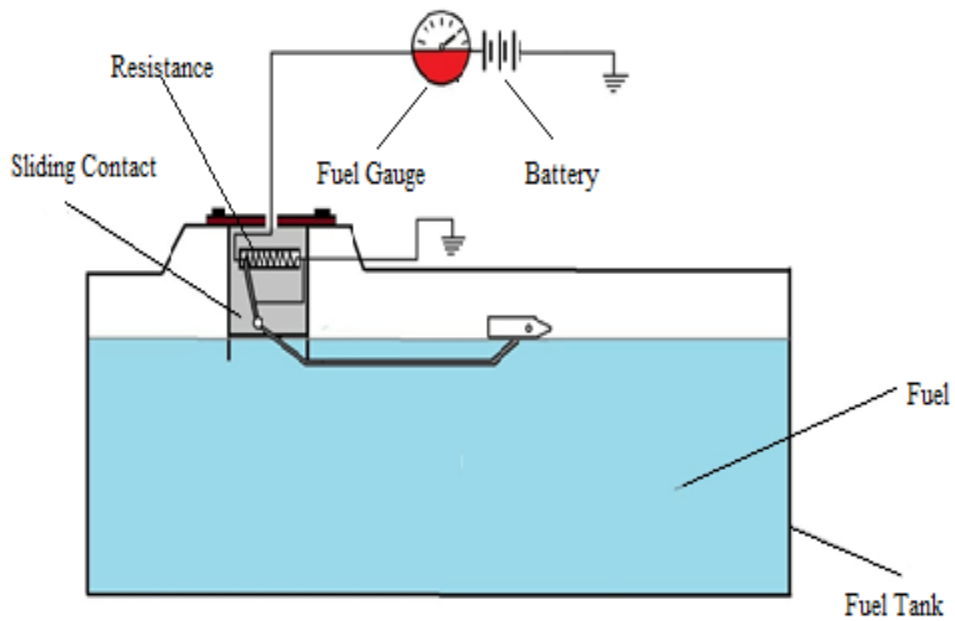


**Figure 2.13**: Block Diagram of Fuel Sending Unit

**Figure 2.14:** EPM 1601 Gas Analyzer

| Table 2.1: Technical Specification of Gas Analyzer EPM1601 | | | |
|---|---|---|---|
| *Measurement Parameter* | *Principle of Measurement* | *Range* | *Resolution* |
| *CO* | NDIR | 0 – 15% | 0.00% |
| *HC* | NDIR | 0– 20000ppm | 1ppm |
| *CO2* | NDIR | 0 – 20% | 0.01% |
| *O2* | Electrochemical | 0 – 25% | 0.01% |
| *NOX* | Electrochemical | 0 – 5000ppm | 1ppm |
| *RPM* | Battery Based | 400 – 9990 | 10 |
| *OT* | RTD | 0 - 150 ℃ | 1 ℃ |
| *Operating Temperature* | | | 0 - 50 ℃ |
| *Measuring Gas Intake* | | | 1 lut/min |
| *Response Time* | | | <5 sec(for sampling probe length of 3m) |
| *Warm-up Time (≥25°C)* | | | 2 min |
| *Zero/Gas Span Calibration* | | | Automatic/Manual |
| *Span Calibration* | | | Digital |
| *Leak Test* | | | Electronic |
| *Power Supply* | | | 12VDC ±2V |
| | | | 230VAC±10%, Single Phase, 50-60 Hz |
| *Power* | | | 25W |

# CHAPTER 3

# CHARACTERIZATION OF WATER ELECTROLYSIS CELL

## 3. CHARACTERIZATION OF WATER ELECTROLYSIS CELL

### 3.1 Introduction

During the last few decades, the addition of hydrogen gas as fuel supplement in internal combustion (IC) engines have fascinated the interests of engineers and scientists worldwide and the interest in this field is still growing. In particular, application of hydrogen gas as fuel supplement for engine performance improvement one area of research under kin the field of hydrogen energy studies (Yilmaz *et al.*, 2010, Arat *et al.*, 2015, Musmar, 2011). These studies have shown that hydrocarbon combustion processes in IC engines requires only specific ranges of HHO gas amount depending on the engine type, fuel and operational conditions   The amount of HHO gas required to improve emission characteristics and performance (specific fuel consumption; fuel economy) on SI internal combustion engine is reported to be around 1/2 or 1/4 of a liter per minute per liter of engine size (Bari *et al.*, 2010; Dulger *et al.*, 2000).  Adding too much amount of hydrogen gas could have negative impact on the emissions, engine life and performance (Yilmaz *et al.*, 2010). In such application of hydrogen gas, among various methods available, alkaline water electrolysis is mostly used for generation of hydrogen in a form called Brown's gas. Due to the high combustible nature of hydrogen and high cost of hydrogen production, on-board electrolysis of water remains at large the best, low-cost, convenient and safest method to produce hydrogen gas for application in internal combustion engine.

However, electrolysis of water process is not 100% efficient due to various factors. Many reports have shown that the electrode material, the space between the

electrodes, the shape of the electrodes, and the type of electrolytes used contribute a significant role in determining the electrolysis efficiency. Platinum (Pt) and gold are reported to highly increase the efficiency of electrolysis; however, because of their high price they are not suitable for both industrial and commercial purposes. The most commonly used electrodes are aluminum, cobalt and nickel. These materials have high resistance to corrosion, high chemical stability and suitable cost and greatly increase the efficiency (Wei *et al.*, 2007). When these electrodes are place close to each other at low current density, the electrical resistance and the formation of bubbles called void fraction decreases, thereby increasing the efficiency. However, at higher current density, the void fraction increases which caused the efficiency of electrolysis to decreases (LeRoy *et al.*, 1979; Nagai *et al.*, 2003). Moreover, since bubbles formation occurs in upper parts of electrodes, greater height of electrode causes more power dissipation in a cell (De Souza *et al.*, 2008, Kaveh *et al.*, 2012). As the separator blocks the movement of the electrolytes, the formation of bubbles also increases when using a separator in a cell causing the electrical resistance to increase three to five times when used without a separator (Nagai *et al.*, 2003; Pickett, 1979). The efficiency is also influence by the nature of the reaction between the electrodes and the electrolytes. Pt reacts much better with KOH electrolyte than Molybdenum (Mo), while 1-butyl-3-methylimidazolium tetrafluoroborate (BMI.BF4) reacts better with Mo than Pt at temperature below ca.333K (De Souza *et al.*,2008). The electrolysis efficiency is also reported to increase with rise in temperature (Nikolic *et al.*, 2012).

The voltage needed to realize alkaline water electrolysis consists largely of reversible potential (= 1.2 V at 25 ℃), overvoltage on electrodes and ohmic loss in

aqueous solution (LeRoy *et al.*, 1979). In actual electrolysis, cell voltage is higher than reversible potential and the difference is converted into heat. Since the reaction is endothermic, heat thus caused is absorbed by the reaction until total cell voltage exceeds 1.48 V, called thermoneutral voltage. This thermoneutral voltage of 1.48V is used as the standard for 100% efficiency. This efficiency is important to know because in on-board water electrolysis application part of the vehicle alternator electrical output will be used to run the electrolyzer unit. For the test vehicle the alternator is rated for 35 Ampere at 13.5-14.4 V.

Therefore, complete knowledge of the operational characteristics of the electrolyzer is necessary to determine the feasibility of applying the technique for on-board hydrogen gas generation. In this Chapter, our experimental investigation on the operational characteristics, and efficiency along with the availability of enough electrical power on board to run the generator at the same time producing enough HHO gas will be presented and discussed.

**3.2 Methodology**

The equipment and measuring instrument used for this experiment are given in detailed in Chapter 2. The cell spacing of the electrolyzer is kept at 1.5 mm while in most other water electrolysis studies the cell spacing used are above 2 mm using 7 cm diameter O ring (Nagai *et al.*, 2003; Mahrous *et al.*, 2011; Mandal *et al.*, 2012). The small cell spacing together with pressure is likely to favor recombination of the product H· and O· radicals back into water molecule. The O rings also limited the surface of the electrolysis to 7cm. Thus all the electrolyte solution within the O-rings are being used and charged with current. This set-up enables maximum electrolysis efficiency. The HHO gas production rate is controlled by either changing the molar

concentration or by adjusting the potentiometer of the PWM. The power supply for electrolysis is obtained from the vehicle alternator. Two 24 A/h is used to reduce loading effect on the alternator: one currently used by the car and the other is installed at the back of the car. The voltage drop across the shunt resistor is used for measuring the current value and voltage is measured by digital voltmeter. The voltage of the vehicle battery along with the measured current is then used for calculating the power energy. The temperature of the electrolytic plates is measured by using MT8530 infrared thermometer and also by placing an alcoholic thermometer at the edge of the plates. The HHO gas production rate is measured by downward displacement of water using a 1 L measuring cylinder calibrated in 10 ml.

The digital multimeter used in the experiment has been seen to hamper the measurement of power consumed due to larger current drawn by the electrolyzer beyond current handling limit of the meter. As a result, shunt resistor is used for all current measurement. A comparison of the current readings within the current holding capacity of the digital multimeter shows that the average deviation between the two ways of current measurements is only 0.44 which is quite small and thus is neglected. These measurement data are shown in **Table 3.5**.

**3.3 Results and Discussions**

**3.3.1 Characterization of a multi-electrode common-ducted HHO dry cell**

For the operation of water electrolyzer on-board electric power will be drawn from the electrical power sources of the vehicle. As a result, understanding the operational characteristics of the electrolyser is essential to investigate the effectiveness of this technique in improving vehicle performance and emission. The parameters studied in this work are HHO gas production rate, electrolyte

concentration, cell voltage, current drawn and temperature dependence in a 3.5x3.5 11-plate HHO Dry Cell at fixed individual cell spacing of 1.5 mm.

Potassium Hydroxide (KOH) and Sodium Hydroxide (NaOH) are the most commonly used electrolyte due to their high conductivity for HHO gas production in water electrolysis. In this work, the interdependence of HHO flow rate, temperature and electrical parameters in alkaline water electrolysis with both KOH and NaOH as electrolytes was investigated.

**Figure 3.1 (a) and (b)** and **Table 3.1** shows the variation of flow rate and power with temperature and the reason why temperature is chosen here as independent variable is that the specific conductivity of the electrolyte depends on temperature (Gilliam, 2007). The gas flow rate increase linearly for both KOH and NaOH as shown in **Figure 3.1 (a) and (b)** and is proportional to temperature. This observation is in agreement with the other reports that the HHO gas production rate increases with temperature (Isao, 2009; Mazloomi *et al.*, 2012, Gilliam, 2007). The linear dependence of gas production rate on temperature is due to the variation of electrolyte conductivity with temperature (Gilliam, 2007). From **Figure 3.1 (a) and (b)**, it can be seen that with increase in temperature, the power consumed increases while the voltage remain almost constant at 11.5 V. Thus, it is observed that the electrical power also increases linearly with temperature.

From **Figure 3.1 (b)**, it can be seen that the power consumption is lower when NaOH is used as an electrolyte. The lower power consumption rate may seem to be beneficial for the vehicle alternator. However, to produce 1.2 LPM of HHO gas, the temperature has to be significantly high. Since temperature and power are interdependent, increasing the temperature will also increase the power consumption

rate. Another method is to increase the molar concentration of NaOH. But even at 2 M, the HHO gas production rate is not sufficient to produce the required amount of HHO gas as can be seen from **Figure 3.2 (Table 3.2)**. Thus the temperature may have to be increase as high as 100°Celsius. However, the acrylic pipe used in the experimental set-up might not be able to withstand such a high temperature not to mention the dangers involve in handling such type of solution.

On the other hand, since KOH has higher HHO gas production rate as compared to NaOH as shown in **Figure 3.1**, the required amount of HHO gas can be easily obtained using low concentration of electrolyte. This beneficial effect of KOH was also reported by Kandah *et al.*, when he compared the HHO gas production rate of KOH and NaCO$_3$ (Kandah, 2014). The higher HHO gas production through KOH as an electrolyte is due to its highest specific conductivity among all alkaline electrolytes (Opu, 2015). Even though the power consumption rate is very high for KOH electrolyte, it can be compensated by using lower molarity concentration of electrolytic solution. Thus according to our experiment, KOH proves a better electrolyte for improving electrolysis efficiency as compared to NaOH.

**Figure 3.3 (Table 3.3)** shows the plot of HHO gas flow rate vs KOH concentration in molarity at 100% PWM duty cycle. The concentration of KOH used in this study varies from 1 to 5 M. It can see from the figure that as the electrolyte concentration increases, the HHO flowrate first increases, reaches a maximum around 0.83 LMP and decreases again. The conductivity is reported to have maximum point at around 6.5 M. The 6.5 M concentration corresponds to 26% (wt/wt), which is the concentration used for most industrial alkaline water electrolysis application (Isao, 2009). The decrease in HHO gas production rate is

due to association of ions at higher concentration. The electric power consumed by the electrolyser also follows the same pattern. This can also be explained according to the dependence of conductivity on electrolyte concentration. When more electrolytes are added, the concentration of ions also increases causing more current to flow through the solution. In **Figure 3.3**, the HHO flowrate appear to lag behind the power for each molarity of the KOH electrolyte. This could happen because when the molarity is increased the conductivity of the electrolyte increase instantaneously while HHO flow rate could not as it depends on temperature of the electrolyte solution which could not increase instantaneously as the supplied power increase. The observed behaviour of the flowrate and power with KOH concentration is in consistent with the variation of KOH specific conductivity with the electrolyte concentration as reported in literature (Gilliam, 2007). According to this report the specific conductivity is not only affected by the concentration of KOH but also by temperature. The rise in temperature is faster as the concentration of KOH increases. Similar trend was also reported by Yuvaraj *et al.* using graphite electrodes (Yuvaraj, 2014). As power and temperature are interdependent, the power consumption rate is seen to increase with temperature. As the molar concentrations increases, the specific conductivity first increases, reaches a maximum value and then decreases. The specific conductivity on the other hand increases linearly with temperature (Gilliam, 2007).

The production of HHO gas, however, has to be controlled for on-board application. In the present study the production of HHO gas was controlled using pulse width modulator (PWM). **Figure 3.4** and **Table 3.4** show the variation of HHO flowrate with PWM duty cycle for 1 M and 2 M of KOH. As the duty cycle is

increased from 20 % to 90%, the flowrate also continues to increase reaching upto 1 LPM for 1 M and 1.38 LPM for 2 M. However, comparing **Figures 3.3** and **3.4** the maximum flowrate attains for 1 M and 2 M are higher in the latter case. This is due to the fact that during flowrate measurements the temperature of the solution is also increasing as the duty cycle is increased which further increases the conductivity of the electrolyte and hence the HHO gas production rate. As the 2 M curve is also smoother for control purpose and has higher production rate of HHO gas, this particular concentration is mostly used in the present study.

**Figure 3.5** and **Table 3.4** show the electrolysis cell voltage for KOH concentration of 1 M and 2 M with respect to the duty cycle. The cell voltage increases as the duty cycle increases for 1 and 2M concentrations. However, it is a bit lower for 2M as compared to 1M solution. This is because the higher the concentration, the smaller is the resistance. That is the presence of larger number of free electrons at higher concentration to increase the conductivity.

The average voltage of the cell during electrolysis at 2 M KOH concentration is 2.4 V which is above the thermoneutral voltage of 1.48 V for alkaline water electrolysis. As all electricity supplied beyond this point will convert into heat, the temperatures of the solutions are found to increase gradually with time during electrolysis (Isao, 2009). As the temperature increase current also increases as shown in **Figure 3.6** and **Table 3.4**. The voltage also continued to increase with temperature. Thus, this observation again shows the linear dependence of current on temperature which is in good agreement with the variation of conductance with temperature as reported by Gilliam *et al.* (Gilliam, 2007). Due to the variation of electrolyte conductivity with temperature, the HHO gas production rate is also found to be

linearly dependent on temperature. The maximum value of HHO gas production rate at 2 M observed is 1.38 $\pm$ 10% LPM at 50.4$^0$ Celsius and 14.63 A.

The effect of Duty cycle on the rate of change of power and temperature at KOH concentrations of 2 M is shown in **Figure 3.7** and **Table 3.4**. As the duty cycle increases, temperature also increases. The maximum HHO flow rate reach in this study is 1.38 $\pm$ 10% LPM at 2 M with maximum power consumption of 175.6 Watt seen at 50.4$^0$ Celsius. At this point the current consumed by the whole electrolyzer unit is measured to be 14.63 A at 12 V. This high power consumption rate can be explained due to the formation of bubbles during electrolysis. As the current density increases, the volume fraction of hydrogen or oxygen bubbles between electrodes called void fraction also increases which in turn increases the electric resistance of the cell causing the efficiency of electrolysis to decrease (LeRoy *et al.*, 1979). The formation of bubbles is quite apparent and is seen on the surface of the plates. Thus, the power efficiency dissipation can be contributed to the bubbles formation during electrolysis.

In water electrolysis, the current or Faraday's efficiency is assumed to be very high reaching almost 100% (Isao, 2009). Therefore the Faraday's efficiency of the alkaline water electrolysis can be approximated by the relation as

$$farday\ efficiency, \varepsilon_f = = \frac{1.23V}{E_{cell}} = \frac{1.23V}{2.34V} \times 100 = 52.56\% \qquad (3.1)$$

However, in actual electrolysis, the cell voltage is higher than the reversible potential because of overvoltages and hence, the thermal efficiency of the alkaline water electrolysis is determined by the thermal efficiency.

$$thermal\ efficiency, \varepsilon_t = \frac{1.48V}{E_{cell}} = \frac{1.48V}{2.4V} \times 100 = 61.67\% \qquad (3.2)$$

Thus the efficiency of our electrolytic system is calculated to be 61.67% at 2M and at $50^0$ C. Our direct measurement has shown that the voltage available at accumulator terminals of the test vehicle is about 14.8 V while the engine is running. This voltage corresponds to applied cell voltage twice the thermoneutral voltage. Therefore if the HHO dry cell is directly integrated with the engine without a current controller, the energy efficiency will be further reduced to 50% and more energy will be lost in the form of heat.

One peculiar property of the 11-plates HHO dry cell electrolyzer is its self-cooling mechanism. This self-cooling mechanism is observed when the HHO dry cell is used in reverse order, that is, the inlet becomes the outlet and vice versa. The self-cooling occurs when the temperature of the solution reaches $65^0$C. During this period, the electrolysis stop and the circulation of electrolyte solution between the dry cell and reservoir tank takes place followed by sudden decrease in the flow rate. After the temperature comes back to $61^oC$, the electrolysis process continues again. For industrial production of HHO gas, this self-cooling seems a beneficial factor as it will help in prevention of overheating of the solution.

## 3.3.2 Feasibility of Applying HHO Generator on- board for Hydrogen Generator in Vehicle Engine

The feasibility of applying alkaline water electrolyzer for on-board hydrogen gas production was determined by comparing the amount of electrical power required and available for producing HHO gas at the flowrate of 1.38 LPM using 2 M KOH concentration. This is the amount flowrate that could be obtained on the maximum side. Regarding the amount of HHO gas required, one thumb rule recommended by some studies and recommended in many commercial sites is 1/4 or

1/2 LMP per liter of the engine capacity to notice improvement in the performance of the test vehicle (Bari *et al.*, 2010; Dulger *et al.*, 2000). That means that, for the present test engine of 796 cc capacity only 0.2 or 0.4 LPM will be required depending on 1/2 or 1/4 respectively. Therefore, according to this rule 1.38 LPM of HHO gas is sufficient for fuel economy.

Regarding the input power source, the test vehicle is equipped with an alternator rated for 35 A at 13.5 to 14.4 volts according to the manufacturer specifications. That is the maximum power the alternator can generate is 472.5 to 504 Watt or 35 Amp at 13.5 to 14.4 volts. But during operation the actual voltage is less than this specification. Assuming the actual operating voltage to be 12V, the total power available will be 420 Watt. **Figure 3.8** and **Table 3.5** shows the power consumed by different electrical components such as headlights, the break light, the indicator and the ON conditions which are 150.4 Watt, 49.6 Watt, 31.2 Watt and 11.2 Watt respectively. Apart from these, the fuel pump is also expected to consume around 192 W at 16 amps and 12 V according to manufacturer specifications. Thus, in total around 300 Watt and about 120 Watt available for the electrolyzer have to be reserved, i.e., about 10 Amp at 12 V. Thus, within this limit, around 0.8 LPM of HHO gas can be produce which is sufficient enough as per the 1/2 or 1/4 rule. But this calculation may not be applicable for all conditions because with increase in number of loads the supply voltage decreases below 12 V. Therefore, according to our observation, HHO production rate upto 0.8 LPM may be accommodated within the power supply system of the vehicle during both daytime and nighttime driving. However, for a flowrate rate of 1.38 LPM and above, application of the electrolyzer

may be feasible during daytime driving only along with 24 AH additional battery power backup.

## 3.4 Conclusions

In this Chapter the electrolyzer was first characterized by investigating the dependence of HHO gas production rate on concentration, temperature, current, duty cycle and cell voltage. Thus it can be concluded that 11 plates HHO dry cell with KOH as electrolyte at 2 M concentration of KOH is enough to produce the amount of HHO gas upto 1.38 LPM which is sufficient enough according 1/2 or 1/4 rule. KOH is found to be better electrolyte than NaOH. At a given concentration of KOH, the HHO production increases with increase in the duty cycle. The observed variations of HHO production rate with the all the above mentioned parameters could be explained based on the variation of the electrolyte specific conductivity with temperature and concentration.

Electrolysis at concentration range of 1 M to 5 M shows that gas flow rate first increases linearly with the concentration and then is found to decrease. This is due to the association of ions at higher concentration. The maximum HHO flow rate reach in this study is 1.38 $\pm 10\%$ LPM at 2 M with power consumption of 175.6 Watt and 50.40 Celsius temperatures. The electrical efficiency of the electrolyzer is estimated to 61.67 % at 159 Watt power consumption.

The electrolyzer is powered by the lead accumulator of 48 AH and the alternator of the test vehicle. The maximum current that can be drawn from the engine alternator is 35 A. Out of this the minimum amount of amperage required to be reserved for all the electrical components of the vehicle is estimated to consume 25 A at 12 V and only about 10 A is available for the electrolyzer. With this amount

of current, about 0.8 LPM of HHO gas can be generated which are sufficient enough for vehicle performance improvement according to 1/2 or 1/4 Rule and our test vehicle engine size. These observations suggested that onboard generation of HHO gas using 11-palte HHO dry cell is feasible if the requirement of HHO gas flowrate is below 0.8 LPM. Above this limit and upto 1.38 LPM requirement of HHO gas, only daytime driving where the headlight is switch OFF is recommended. Other options available to make more room for water electrolysis in terms of electrical energy in the test vehicle are

a) Replacement of all the lighting components by LED systems as the latter is more energy efficient than the former one.

b) Upgrading the alternator to higher amperage one.

From these report it can be seen that there is a strong need to increase the efficiency of alkaline water electrolysis process for onboard generation of hydrogen gas. An efficiency of 61.67 % is not good enough to see the impact of larger HHO flowrate. On the other hand, the data and results documented in this thesis are expected to be helpful for those who are using and planning to use these type of HHO Dry Cell or similar type.

**List of Figures**
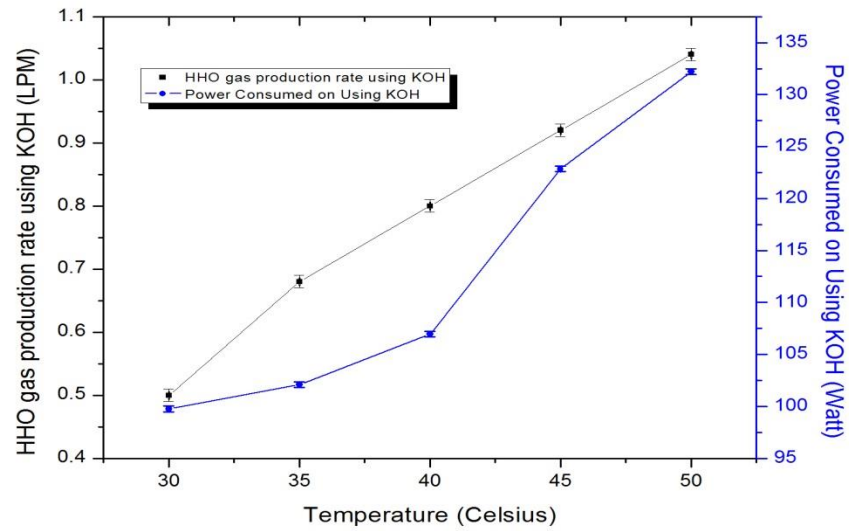


**(a)**
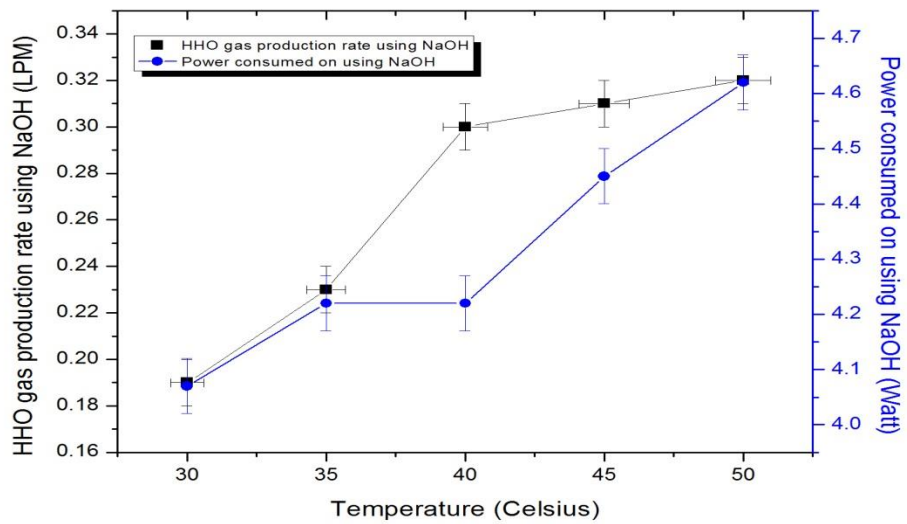


**(b)**

**Figure 3.1: a)** Variation of Temperature on KOH-HHO gas production rate

**b)** Variation of Temperature on NaOH-HHO gas production rate

48
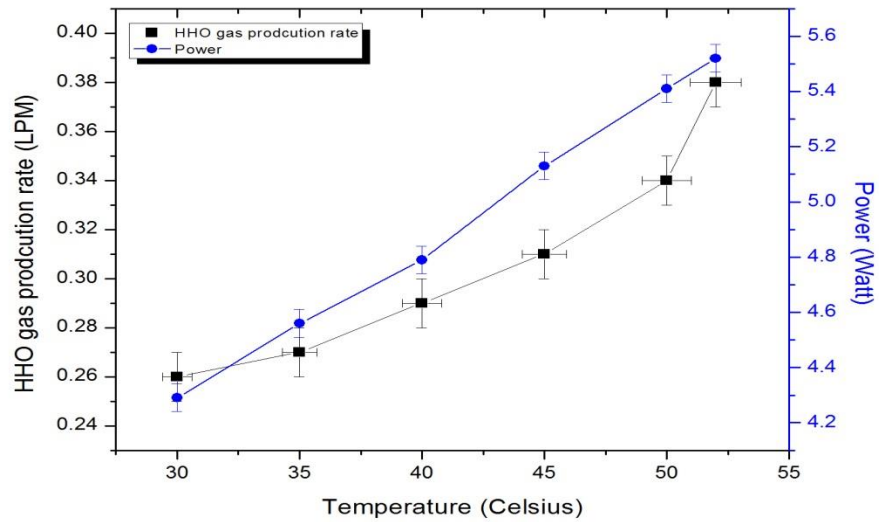
**Figure 3.2:** NaOH-HHO gas production Rate at 2 M
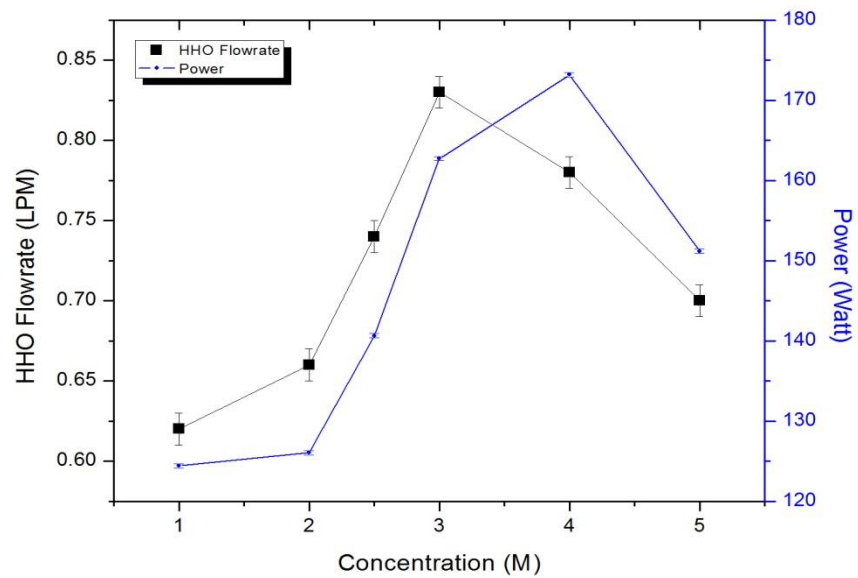


**Figure 3.3:** Variation of HHO gas flow rate (liter per minute) with KOH concentration (M)
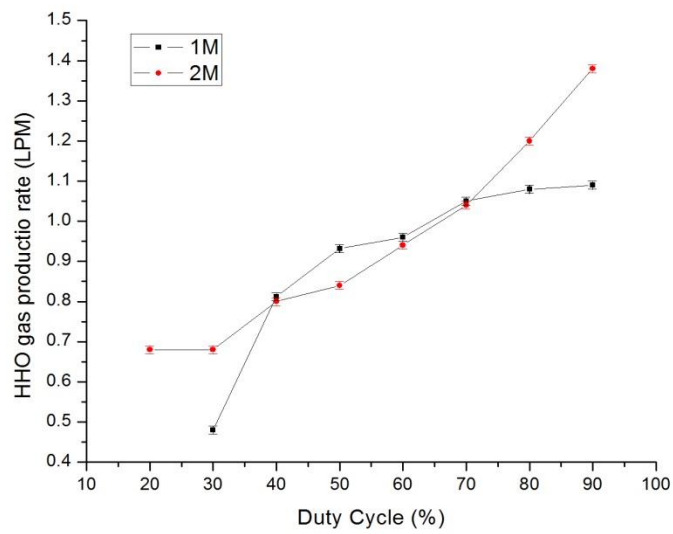
**Figure 3.4:** Effect of Duty Cycle of PWM on HHO gas production rate at KOH concentrations 1 M and 2 M.
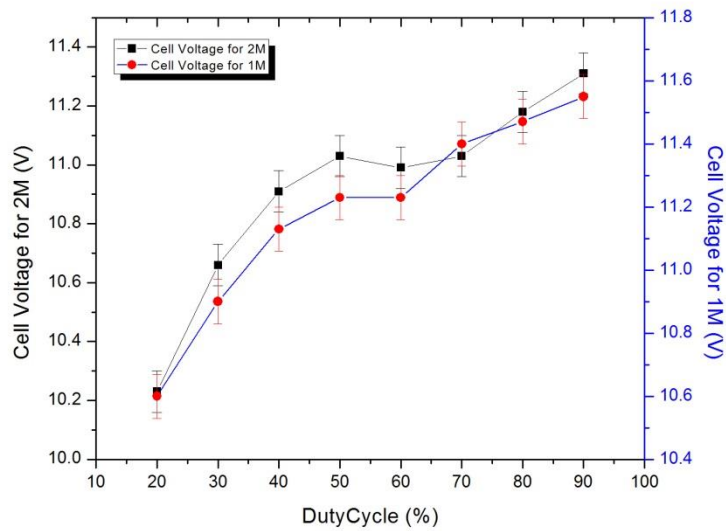


**Figure 3.5:** Variation of Cell Voltage with Duty Cycle at 1 M and 2 M concentrations of KOH
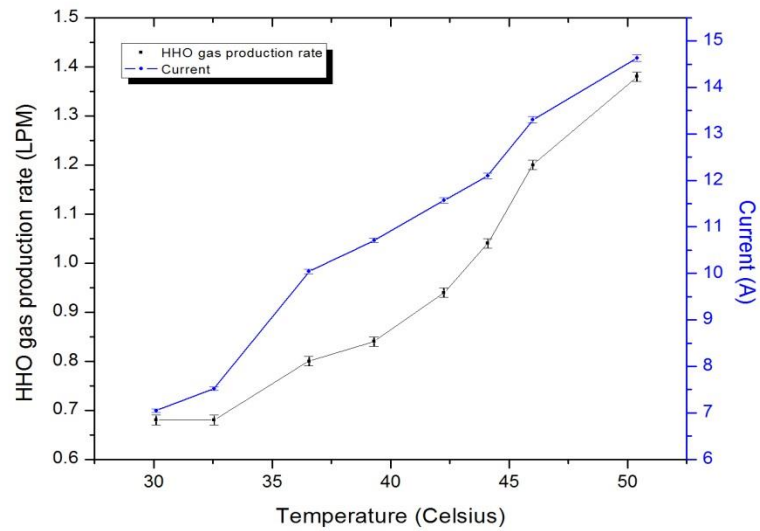
**Figure 3.6:** Variation of HHO production rate and Current with Temperature at 2 M

KOH as electrolytes
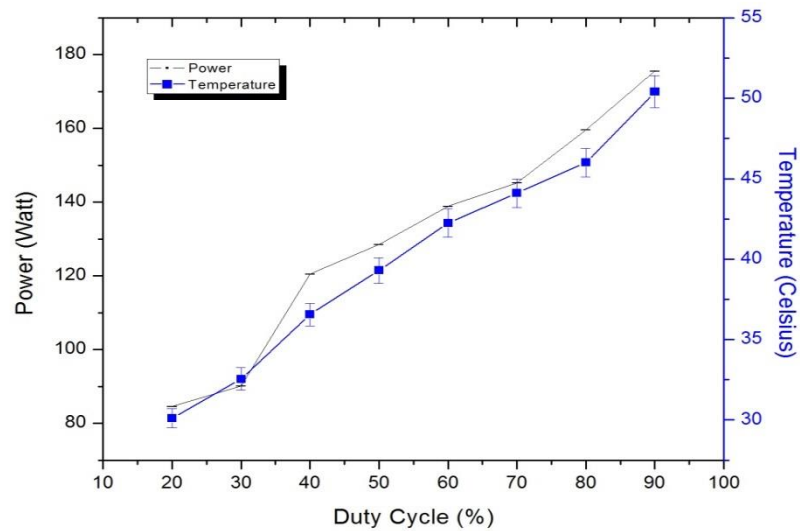


**Figure 3.7:** Effect of Duty cycle on electrical power consumed (Watt) and

temperature (Celsius) at KOH concentrations of 2 M.
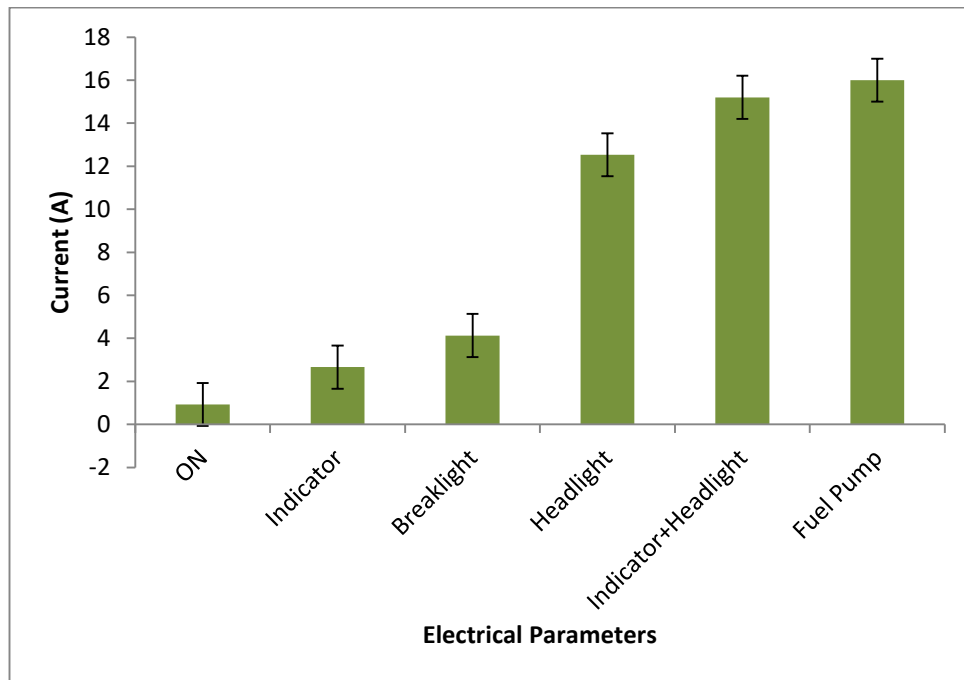
**Figure 3.8:** Electrical load of different electrical components of the test vehicle.

## List of Tables

| Table 3.1: HHO flow rate, temperature and electrical parameters in alkaline water electrolysis with both KOH and NaOH as electrolytes | | | | | | | | | | | | |
|---|---|---|---|---|---|---|---|---|---|---|---|---|
| 1 M of KOH | | | | | | | 1 M of NaOH | | | | | |
| Temperature | | HHO gas production rate using KOH | | Current | Voltage | Power Consumed on Using KOH | | HHO gas production rate using NaOH | | Current | Voltage | Power consumed on using NaOH | |
| Celsius | Error (±) | LPM | Error (±) | (A) | (V) | (A) | Error (±) | LPM | Error (±) | (A) | (V) | Watt | Error (±) |
| 30 | 0.02 | 0.5 | 0.01 | 8.8 | 11.6 | 99.8 | 0.27 | 0.19 | 0.01 | 0.36 | 11.3 | 4.1 | 0.27 |
| 35 | 0.02 | 0.68 | 0.01 | 8.6 | 11.6 | 102.1 | 0.27 | 0.23 | 0.01 | 0.37 | 11.4 | 4.2 | 0.27 |
| 40 | 0.02 | 0.8 | 0.01 | 9.3 | 11.5 | 106.9 | 0.27 | 0.3 | 0.01 | 0.37 | 11.4 | 4.2 | 0.27 |
| 45 | 0.02 | 0.92 | 0.01 | 10.5 | 11.7 | 122.9 | 0.27 | 0.31 | 0.01 | 0.39 | 11.4 | 4.5 | 0.27 |
| 50 | 0.02 | 1.04 | 0.01 | 11.3 | 11.7 | 132.21 | 0.27 | 0.32 | 0.01 | 0.40 | 11.5 | 4.6 | 0.27 |

Note: table header has 14 columns but body has different count; reproduced as read.

| Table 3.2: HHO flow rate, temperature and electrical parameters in alkaline water electrolysis with 2 M NaOH as electrolytes | | | | | | | |
|---|---|---|---|---|---|---|---|
| Temperature | | Current | Voltage | Power | | HHO gas production rate | |
| (Celsius) | Error(±) | (A) | (V) | (Watt) | Error(±) | (LPM) | Error(±) |
| 30 | 0.02 | 0.38 | 11.3 | 4.29 | 0.27 | 0.26 | 0.01 |
| 35 | 0.02 | 0.4 | 11.4 | 4.56 | 0.27 | 0.27 | 0.01 |
| 40 | 0.02 | 0.42 | 11.4 | 4.79 | 0.27 | 0.29 | 0.01 |
| 45 | 0.02 | 0.45 | 11.4 | 5.13 | 0.27 | 0.31 | 0.01 |
| 50 | 0.02 | 0.47 | 11.5 | 5.41 | 0.27 | 0.34 | 0.01 |
| 52 | 0.02 | 0.48 | 11.5 | 5.52 | 0.27 | 0.38 | 0.01 |

| Table 3.3 : HHO flow rate and Power Consumed at different concentrations of KOH | | | | | |
|:---:|:---:|:---:|:---:|:---:|:---:|
| Concentration | | HHO Flowrate | | Power | |
| M | Error(±) | LPM | Error(±) | Watt | Error(±) |
| 1 | 0.01 | 0.62 | 0.01 | 124.4 | 0.26 |
| 2 | 0.01 | 0.66 | 0.01 | 126. | 0.26 |
| 2.5 | 0.01 | 0.74 | 0.01 | 140.7 | 0.26 |
| 3 | 0.01 | 0.83 | 0.01 | 162.7 | 0.27 |
| 4 | 0.01 | 0.78 | 0.01 | 173.2 | 0.27 |
| 5 | 0.01 | 0.7 | 0.01 | 151.2 | 0.26 |

**Table 3.4:** HHO gas production rate at different duty cycle of PWM. The uncertainty in HHO Flowrate Measurement is ±0.01

| | | | 20 | 30 | 40 | 50 | 60 | 70 | 80 | 90 |
|:---:|:---:|:---:|:---:|:---:|:---:|:---:|:---:|:---:|:---:|:---:|
| Duty Cycle (%) | | Error (±) | 0.01 | 0.01 | 0.01 | 0.01 | 0.01 | 0.01 | 0.01 | 0.01 |
| 1 M | Temperature | Celsius | 35 | 37 | 43 | 49 | 54 | 56 | 59 | 60 |
| | Current | A | 4.39 | 6.25 | 8.25 | 9.09 | 10.11 | 10.51 | 10.82 | 11.57 |
| | | Error (±) | 0.02 | 0.03 | 0.04 | 0.05 | 0.05 | 0.05 | 0.05 | 0.06 |
| | Voltage | V | 10.59 | 10.9 | 11.12 | 11.23 | 11.23 | 11.39 | 11.47 | 11.55 |
| | | Error (±) | 0.07 | 0.07 | 0.07 | 0.07 | 0.07 | 0.07 | 0.07 | 0.07 |
| | HHO gas Production rate | L/min | - | 0.48 | 0.81 | 0.93 | 0.96 | 1.05 | 1.08 | 1.09 |
| | | Error (±) | - | 0.01 | 0.01 | 0.01 | 0.01 | 0.01 | 0.01 | 0.01 |
| | Power | Watt | 46.5 | 68.1 | 91.8 | 102.1 | 113.5 | 119.8 | 124.8 | 133.7 |
| | | Error (±) | 0.06 | 0.08 | 0.08 | 0.09 | 0.09 | 0.09 | 0.09 | 0.09 |

| | | | | | | | | | | | |
|---|---|---|---|---|---|---|---|---|---|---|---|
| 2 M | Temperature | Celsius | 30.1 | 32.55 | 36.55 | 39.3 | 42.25 | 44.1 | 46 | 50.4 |
| | Current | A | 7.05 | 7.52 | 10.04 | 10.71 | 11.57 | 12.1 | 13.3 | 14.63 |
| | | Error (±) | 0.04 | 0.04 | 0.05 | 0.05 | 0.06 | 0.06 | 0.07 | 0.07 |
| | Voltage | V | 11.99 | 11.99 | 12 | 11.99 | 12 | 12 | 12 | 12 |
| | | Error (±) | 0.07 | 0.07 | 0.07 | 0.07 | 0.07 | 0.07 | 0.07 | 0.07 |
| | HHO gas production rate | L/min | 0. 68 | 0.68 | 0.8 | 0.84 | 0.94 | 1.04 | 1.2 | 1.38 |
| | | Error (±) | 0.01 | 0.01 | 0.01 | 0.01 | 0.01 | 0.01 | 0.01 | 0.01 |
| | Power | Watt | 84.6 | 90.2 | 120.5 | 128.5 | 138.9 | 145.2 | 159.6 | 175.6 |
| | | Error (±) | 0.08 | 0.08 | 0.09 | 0.09 | 0.09 | 0.09 | 0.1 | 0.1 |

| **Table 3.5:** Electrical load of different electrical components of the test vehicle | | | | | |
|---|---|---|---|---|---|
| Parameters | Shunt Resistor Voltage (mV) | Current | | Voltage (V) | Power (Watt) |
| | | (A) | Error (±) | | |
| ON | 0.7 | 0.93 | 0.01 | 12 | 11.2 |
| Indicator | 2 | 2.66 | 0.02 | 12 | 31.9 |
| Breaklight | 3.1 | 4.13 | 0.03 | 12 | 49.6 |
| Headlight | 9.4 | 12.53 | 0.08 | 12 | 150.4 |
| Indicator+Headlight | 11.4 | 15.2 | 0.09 | 12 | 182.4 |
| Fuel Pump[*] | | 16 | | | |

[*]* As per specification given in the product.

# CHAPTER 4

# EFFECT OF HHO GAS ON THE PERFORMANCE AND EMISSION CHARACTERISTICS

# 4. EFFECT OF HHO GAS ON THE PERFORMANCE AND EMISSION CHARACTERISTICS

## 4.1 Introduction

From Chapter 3, it can be seen that maximum of about 1.38 LPM of HHO can be generated from on-board water electrolyser consisting of 11- multiple electrodes HHO Dry Cell at an electrical energy efficiency of 61.67%. At this HHO gas production rate, the current drawn by the electrolyser unit is about 14.63 A which could be accommodated on the maximum side without much engine loading and making use of an additional 24 AH lead accumulator. The present chapter reports the effectiveness of this much amount of HHO gas in the performance of a test vehicle in terms of mileage and emission characteristics.

According to earlier and recent studies on the application of hydrogen or HHO gas as fuel supplement, hydrogen or HHO has been shown to have improvement in engine torque, brake thermal efficiency, specific fuel consumption and emission characteristics. Several studies (Dulger *et al.*, 2000; Uykur *et al.*, 2001; Bari *et al.*, 2010) have shown that application of Brown's gas in a gasoline/diesel generator or automobile engine can significantly improve engine emissions, performance and fuel efficiency. Hydrogen addition is also reported to improve the brake thermal efficiency, combustion characteristics, lean burn limit and reduced $CO_2$ and HC emissions of gasoline SI engines. The thermal efficiency increase with increase in hydrogen content and is reported to be around 2–31.56% (Ganesh *et al.*, 2008; Edward *et al.*, 2003; Ceviz *et al.*; Ji and Wang, 2009). On the other hand the low volume density of hydrogen was also reported to reduce torque output of

hydrogen engine as compared to pure gasoline engine (Sopena *et al.*, 2010). Moreover, because of high combustion temperature increase in $NO_x$ emissions was observed. The increase in $NO_x$ emissions is due to oxidation of nitrogen in air at high temperature. Recirculation of exhaust gas and retarding the combustion by introducing the exhaust gas into the cylinder will cool and slow down the combustion rate of the engine thereby reducing the $NO_x$ emissions in conventional engines (Du *et al.*, 2017). Lean burn condition can also reduce the $NO_X$ emission level by 94% (Edward *et al.*, 2003).

However, most of these reports were based on experimental results obtained from engine test rigs or stationary engines, and it is not known to what extend these laboratory results could be applicable in vehicular system during actual road transport. One of the official reports that can be seen is Dulger *et al.* according to which HHO fuel supplementation increases the fuel economy of a vehicle by 33% (Dulger, 2000). But this paper does not clearly mention how mileage is measured. Therefore, it is not known whether the same amount of improvement can be achieved with HHO gas addition in a vehicle during real time on-board transportation under the influence of power loses from crank shaft to wheel of a vehicle.

Mileage is the distance travelled by a motor vehicle per unit amount of fuel consumed and it is an important performance index parameter which is directly related with the fuel economy. It is measured either in km/L or L/km. In automobile manufacturing industries, mileage specification is obtained through a series of measurement using Chassis Dynamometer under controlled conditions for some few driving cycles. However, the actual mileage achieved by vehicle in during actual road transport applications generally could not meet the specifications. This is due to

the fact that the Laboratory measurement cannot take into account variation in conditions like road condition, driving style, traffic conditions, fuel quality used and load taken. It is, therefore, important to have a better means of mileage measurement which can provide actual mileage average value under any driving conditions. Most modern passenger cars are provided with Trip Meter to indicate the average as well as real time mileage values. However, commercial vehicles manufactured before 2006 were hardly equipped with such facilities. Therefore, method is needed which could reveal the actual mileage of the vehicle under the influence of real environment.

Apart from chassis dynometer some of the other techniques that have been used in mileage measurement are

(i) Electronic Control Unit (ECU): By retrieving mileage related data from the vehicle ECU using a diagnostic tool.

(ii) Fuel consumption rate meter: By fitting these commercial meters in the inlet and return fuel line, amount of fuel consumed can be measured.

(iii) Emission Data: Exhaust emission data of CO2 can be used to estimate the amount of hydrocarbon fuel consumed, but the accuracy may not be high as it depends on the assumption that all HC fuel consumed is completely converted into $CO_2$.

The above methods are all basically work on the real time electrical signal generated by sensors and , as a result S/N ratio of the may be low due to interference from noise and spike. Moreover, these methods required special scientific tools with technical skill which may be disadvantageous in some situations. Therefore, a simpler but reliable technique for fuel consumption measurement is needed for knowing the true average mileage of a vehicle. Through the present work, a new fuel

consumption measurement method is developed making use of the fuel level indication system of a vehicle.

## 4.2 Methodology

The quest for simple and cheap method for accurate measurement leads us to the investigation of three closely related methods of calibrating the fuel sender unit (FSU):

A) The Voltage Drop method

B) The Linear Resistance method

C) The Polynomial Resistance Method.

For calibrating the fuel sender unit, the test vehicle is first positioned horizontally and the fuel in the tank is piped out as much as possible from the fuel tank. Then the fuel is added back in step of 1 L each, and the change in voltage or resistance are measured across the fuel sender unit resistor. This step is continued till the fuel tank is full. A simplified typical example of fuel level indicator system and its electrical connection used in commercial vehicle is given in **Figure 4.1.**

In voltage drop method, the voltage drop across the FSU is correlated with the amount of fuel added during which the electrical system is required to be switch on.

In the Linear Resistance Method (LRM) and the Polynomial Resistance Method (PRM) **(Figure 4.1)**, resistance is the parameter measured from the FSU and the vehicle can be put in switch off mode. The main difference between Linear Resistance Method and the Polynomial Resistance Method is whether the fuel sender unit is connected to the fuel gauge or not. It is disconnected in the latter method.

The HHO gas is directly added to the engine cylinder through the air filter via a plastic pipe. **Figure 4.2** shows the block diagram of how HHO gas is applied to the engine. This is the most common and easiest way of introducing HHO gas to the engine combustion cylinder. No other modification is made in the engine system. To reduce loading effect on the engine by the electrolyzer unit, an additional 24 AH battery source is included in the power supply system. The power supply first enters the PWM where the amount of current applied to the HHO generator is controlled by its duty cycle. When power supply enters the HHO dry cell, electrolysis occurs that results in the production of HHO gas. The HHO gas is then taken out from the reservoir tank and feed to bubbler via a flashback arrestor valve. The bubbler prevents backfire as well as help in removing the water vapor present in the HHO gas. Before the bubbler two flashback arrestor valves are connected in series. The HHO gas is then taken out from the bubbler and supplied to the engine through the air filter.

In order to measure specific fuel consumption of the test vehicle dynometer is required which is not available in the institution and hence cannot be done at this moment to know the effect of the electrolyzer in terms of specific fuel consumption. Instead two 24 Ah lead accumulator were used to reduce loading by the electrolyzer on vehicle power system. Therefore, the power loading effect of the electrolyzer on the engine fuel consumption was considered to be small compare to other causes such as traffic condition, road condition.

Mileage of a vehicle can be affected by a number of factors such as driving style, road conditions and speed. To minimize the effect of these factors, mileage measurements were conducted throughout this experiment using the same driver, same road condition, same distance travelled and in the speed range 25-30 km/hr.

The quality of petrol is also kept constant. The road condition chosen for the mileage measurement include uphill and downhill.

The tail pipe emissions of the vehicle under study is measured using i3 Sys Gas Analyzer EPM1601 which is in compliance with BAR-97, OIML class 0 and ISO3930 international standards, Indian Standard CMVR/TAP-115/116 issued by Ministry of Road Transport & Highways. The EPM1601 required warm up time of two minutes after which it performs self-diagnostic test like leak check and zero error. The vehicle settings are done to select the type of vehicle, petrol and number of cylinder used. After the vehicle settings, self-diagnostic hydrocarbons residue check is done and the engine of the vehicle is turn on and then accelerated for 20 seconds. The engine is then returned to idle position/neutral position and the sampling probe of length 7 cm of the EPM1601 gas analyzer is inserted to the tail pipe of the vehicle under study. The exhaust emission characteristic is observed and recorded either through display screen of the gas analyzer or the laptop that is interfaced with the gas analyzer using XCTU software.

## 4.3 Results and Discussions

### 4.3.1 Calibration of Fuel Sending Unit

**Figure 4.3 and Table 4.1** shows the results of fuel sender unit calibration in voltage drop method. The relationship between the voltage drop and the amount of petrol added can be best fitted with linear curve. In this method, the electrical system of the engine has to be switch ON during the whole process of calibration. As a result, towards the end of each experiment the battery voltage of the vehicle becomes low such that the observed data deviates from what would be expected under fully charged battery. The effect of the low battery voltage is seen in the extremity of x-

axis of **Figure 4.2 (a)** as a distorted region. Thus, in voltage drop method, the observed data towards the end of each experiment has to be neglected. Only the initial and mid-data of the experiment shows a linear relationship between the petrol added and the voltage drop as shown in **Figure 4.3(b)**. The equation describing the relation between Voltage vs Fuel added can be approximated by

$$y = 0.11x + c \qquad\qquad (4.1)$$

The intercept c varies from one calibration set to another due to difference in the initial fuel level used while the slope almost remains constant. From the above relation it can be seen that for every 1 L change in amount of petrol in the fuel tank, there is a voltage drop of 0.11 V, that is, for 1 V change in voltage drop, 9.09 L of petrol has to be added. This is quite a big amount indicating the low sensitivity of the method and was rejected for further mileage measurement.

In Linear Resistance Method, the electrical system of the vehicle is switched OFF and the resistance of the FSU is recorded with each litre of petrol addition and the corresponding graph between the observed resistance and petrol addition is plotted. **Figure 4.4** shows the variation of observed resistance ($\Omega$) and fuel level in the tank.

The measurement of the resistance of the test vehicle per one liter of petrol shows that as the amount of petrol is increasing the resistance starts decreasing linearly indicating that the level of petrol in the vehicular fuel tank has an inverse relationship with the fuel sender unit (FSU) resistance. The calibration is repeated a number of times and are shown in **Figure 4.5 (Table 4.2)**. It can be seen that the

linear fitting is much better compared to voltage drop method and is described by the equation

$$y = 0.89x + 36.49 \qquad (4.2)$$

All the curves have almost the same slope value but different values of intercept as given in **Table 4.3.** The variation in the intercept is due to difference in the initial fuel level in each calibration set. But for fuel consumption measurement the most important parameter is the slope and variation in the intercept value does not matter in further estimation. The average slope of the linear fits is about 0.89 L/R with $R^2 = 0.99$ **(Table 4.3)**. This means that to get a change in resistance of 1 $\Omega$, 0.89 L of petrol has to be added. This slope value is used to determine the amount of fuel consumed and hence the mileage as follows

$$Mileage = \frac{Distance\ travelled}{Fuel\ Consumed(l)} = \frac{Distance}{(R2-R1)/\ slope} Km/L \qquad (4.3)$$

where R1 and R2 are the FSU resistance before and after a trip.

The average value of mileage using Linear Resistance Method is calculated to be 14.58 km/L at a speed of 25- 30 km/hr **(Table 4.4)** which is very closed to the city mileage value of 13 km/L specified by the manufacturer. However, this technique is associated with the problem of high resistance reading right after a trip is completed. This problem arises due to the fact that the fuel gauge coil is in parallel electrical connection with the fuel sender unit resistor. So, current flows through these units during a trip which heats up the coil and resistor and hence changes the resistance value. Thus, the vehicle has to be allowed to cool down for at least 30 min before recording the resistance measurement.

Polynomial Resistance Method (PRM) is developed to remove the disadvantages of the Linear Resistance Method (LRM) at the same time retaining all the beneficial properties of LRM. In PRM, the connection between the fuel sender unit and the fuel gauge is opened. After disconnection, the resistance that was measured is simply the resistance of the isolated fuel sender unit resistor. The resistance value for an empty fuel tank is measured to be 117.4 $\Omega$ as given in **Table 4.5**. The plot of resistance change with addition of petrol gives polynomial graph as shown in **Figure 4.5 (Table 4.6)** and can be described by the equation

$$y = 28.33 + 0.42089R + 0.00177R^2 \qquad (4.4)$$

Using this equation, the amount of fuel consumed can be estimated as

*Amount of petrol consumed, l= R2-R1\*{[(R2+R1)\*1.77]-420.89}* (4.5)

where R2= final resistance value, R1=initial resistance value, and the constant numerical values gives the coefficient of $a_1$ and $a_2$ for each litre of petrol addition respectively

With this technique the average city mileage at a speed of 25- 30 km/hr of the test vehicle is calculated to be 18.86 km/L. It was found that polynomial fitting is applicable to all the observed data whether it is in the mid-region or the upper, and even a change of  0.5 L of fuel can be measured.

**4.3.2 Effect of HHO gas on Fuel Economy**

**Figure 4.7 and Table 4.7** gives a detailed account of the effect of HHO gas on the fuel economy or the mileage of the test vehicle without any modification to the engine. The amount of HHO gas applied is 1.38 LPM which consumed a current of 14.36 A. The average mileage of the vehicle without HHO is 18.86km/L. Out of 7 test runs at the speed of 25-30 km/hr, the 6 test shows mileage improvement while 2

tests is negative.  That means 71 % success rate. The maximum mileage gain is 11.08% and minimum mileage gain of 0.48%. The improvement in mileage can be attributed to the high combustion velocity of HHO. Thus, all the fuel detonates all the fuel at once thereby putting more pressure on the piston in a shorter time interval and extracts more power from the fuel.

The loss fraction in the above test runs arises from traffic jam which prevents us from keeping up with the test speed range. However, during this period the lambda sensor of the test vehicle still working trying to maintain a constant air-fuel ratio (AFR) of 14.7:1, that is, 14.7 parts of air to 1 part of fuel. As a result, in congested traffic the extra oxygen due to HHO gas will cause unnecessary increase in fuel consumption that leads to the loss in mileage. The AFR is adjusted by the information relayed by the lambda sensor and prevents too rich (more fuel) and too lean (more air) air-fuel mixture. This mechanism is most effective in idle engine running condition.

Effect of HHO with engine system modification by disabling the Lambda Sensor is also investigated. **Figure 4.8** shows the HHO gas effect without the lambda sensor. After this modification, the effect of HHO gas appears more clearly. The average mileage of the vehicle without HHO and lambda sensor is 16.46km/L.  In all the 5 test runs, mileage improvement were observed in the range 13.2-27.96 with the average mileage gain of which is 19.79%. The high gain in mileage without the lambda sensor can be explained on the basis of carbureted engine system. Without the lambda  sensor, the vehicle engine acts as a carbureted engine and the amount of petrol consumed is not maintained to a specific value, but depends on the demand of the driving condition, that is, mainly on the engine RPM. As there is no lambda

sensor to compensate for the extra oxygen in HHO gas, the fuel is burned effectively and efficiently by the HHO gas resulting in lower fuel consumption rate and hence greater mileage gain.

The overall mileage gain- including the loss, with and without lambda sensor is 11.32%. The beneficial effect of HHO gas in the test vehicle is also seen from the engine revolutions per minute (RPM). Since the HHO generator is on board, one of the crucial parameters to determine the effect of HHO gas depends on Revolutions Per Minute (RPM). The engine RPM without HHO is around 3500 on upward run and 1640 on downward slope. When HHO gas of 2 Molarity at 1.38 LPM with current consumption of 14.63 A is supplied to the engine, the engine RPM is 3040 on upward slope and 1640 on downward slope. This observation is also confirmed by the driver based on lower acceleration on upward slope when using HHO gas. Thus, the shorter burning duration and wider flammability range of HHO-gasoline blends improve the combustion efficiency.

From **Figure 4.7** and **Figure 4.8**, there is a large variation in mileage in the experimental data. This anomaly can be attributed to change in traffic condition and the corresponding driver reaction to it, which result in variation of the driving speeds. Thus, the mileage obtained is greatly influenced by the traffic condition when using HHO gas with or without the lambda sensor. Hence, in this thesis, the mileage of the test vehicle is studied in statistic mode.

### 4.3.3 Effect of HHO Gas on the Emission Characteristics

The effect of HHO gas on the emission characteristics of Maruti was studied using i3sys Gas Analyzer EPM1601. The uncertainty in emission measurement for

all gases is ±5 %. The effect of HHO gas at lower KOH concentration of 1.5 M was studied at different duty cycle under idle condition. The emission characteristics of the test vehicle without HHO are 0.13 % for CO, 69.23ppm for HC and 14.34% for $CO_2$ for this particular experiment. When HHO gas is added, the emission of HC and CO first decreases to a minimum and then increase again with increasing value of duty cycle. The maximum improvement in CO emission is 23.07% seen at 50% duty cycle and for HC, an improvement upto 6% is observed at 30% duty cycle as given in **Figure 4.9** and **Table 4.8**. This observation indicates the existence of optimum point for HHO gas at which the HC and CO emission improvement reach maximum. Beyond this point the emitted concentrations of the above gases increase again.

*i) Emissions Characteristics with lambda sensor*

At 2 M KOH concentration and 1.38 LPM HHO flowrate, CO emission continue to show improvement by 13.38 %  as shown in **Figure 4.10 (Table 4.9)** while HC emission is observed to increase by 7.57% **(Figure 4.11 and Table 4.9)**. At this gas flowrate, the water vapour content of the HHO gas is also high as can be detected visually. It may be possible that the water vapour entering the cylinder in some way or other prevents complete combustion of the HC fuel by lowering combustion temperature or inhibiting the oxidation reaction of the fuel. As a result of the conversion of CO to $CO_2$, the emission characteristic of $CO_2$ is inversely proportional to that of CO emission. Hence, carbon dioxide ($CO_2$) emission was found to increase with the application of HHO gas. The increase in HC and $CO_2$ emissions can be attributed to the fact that a low speeds; low lean-flammability limit prevents hydroxy gas to have positive influence on combustion efficiency due to mixture requirement around stoichiometric conditions.

Thus, under idle condition, HHO gas has the effect of reducing CO emission level while it increases HC concentration. A slight emission of nitrogen dioxide was found during the acceleration and at the initial stage of cold start. In all the above cases, $CO_2$ emission increases confirming the occurrence of better engine combustion in the presence of HHO gas fuel supplement. It appears that HHO gas is most effective in reducing CO only but not HC. This is because when HHO gas is added, due to its high flame speed, CO molecules will be burned first for being simpler molecule than HCs leading to the observed decrease in CO emission. At the same, HC emission is also expected to decrease as a result of completion combustion, but our result is in contrary to that and to other reports. This is attributed to effect of water form by HHO combustion on the catalytic converter because the other reported work on application hydrogen or HHO gas as fuel supplement were conducted mostly on engine test rig which does not have catalytic converter.

*ii) Emissions Characteristics without lambda sensor*

**Figure 4.12 (Table 4.10)** shows the emission characteristics of CO and $CO_2$ without the lambda sensor in the test vehicle. The HHO gas supplied as fuel supplement is 1.5 M KOH concentration at 100% duty cycle with current consumption of 11.2 A. The CO emission is again found to decrease by 10.76%. However, an average increase of 2.03% is observed in the $CO_2$ emissions (**Figure 4.12)** and the HC emissions increased by 2.45% with the application of HHO gas **(Figure 4.13 and Table 4.10)**. An important point to note without the lambda sensor is the observation of the emissions of Nitrogen Oxide ($NO_x$). In **Figure 4.13**, the emissions level of NOx is increased by 7.75% when HHO gas applied to the test

vehicle. The appearance of NOx emission is attributed to higher combustion temperature in the presence of HHO gas. This observation is in contrast to some other reports that the addition of HHO gas to gasoline fuel reduces $NO_x$ emissions. This can be attributed to lean burn condition when the lambda sensor is removed. This leads to increase in temperature which in turn increases the $NO_x$ emissions. Comparison of emission data without HHO gas shows that apart from appearance of NOx, the emission levels of CO decreased by 10.76%, while the HC and $CO_2$ emissions increased by 2.03% and 2.45% respectively. Moreover, comparing the emission levels with and without the lambda sensor, it can be seen that the sensor alone could reduce the CO and HC emissions by about 90% and 56% respectively at the same time reducing NOx beyond detectable value from 153 ppm. These observations indicated that the lambda sensor used in vehicle is effective enough in controlling the emission level of HC, CO and NOx than the HHO gas fuel supplement.

## 4.4 Conclusions

In this chapter the experimental results of HHO gas introduction as fuel supplement are presented and discussed. The fuel tank of the vehicle is calibrated to determine the actual amount of fuel consumed by the engine using three methods namely: The Voltage Drop Method, The Linear Resistance Method and The Polynomial Resistance Method. Out of these, LRM and PRM give best results but in terms of reliability PRM was recommended and used for mileage measurement throughout this work. The uncertainty in mileage measurement using this method is estimated to be within 10%.

In mileage measurement, out of 7 test runs for 10.1 km at the speed of 25-30 km/hr, the 6 test shows mileage improvement while 2 tests is negative. That means 71 % success rate. The highest mileage gain achieved is 27.96% and is observed without the lambda sensor while the highest mileage gain with the lambda sensor is 11.08%. One point to note in mileage measurement is that the HHO generator is continuously running whether the road condition is uphill or downhill. During downhill driving, the mileage value of the vehicle reached its maximum value and HHO addition may not have appreciable effect under which the electrolyzer can become power consumer only. Thus, if the generator is switched off during downward trip, the improvement chances and mileage value are also expected to be higher.

On the average the mileage with and without Lambda sensor are respectively 18.86 and 16.46 KM/L and it is slightly better with the Lambda sensor. This is what is expected as Lambda sensor maintains constant Air/Fuel ratio for better mileage. However, when HHO gas is injected the Lambda sensor will detect the presence of more oxygen content which will instruct the vehicle computer to inject more fuel to maintain correct A/F ratio as before. On the other hand, when Lambda sensor is remove the increased oxygen level in the exhaust on HHO addition will not be detected and the amount of fuel inject will not increase as before. As a result, the mileage gain becomes higher with HHO gas addition without lambda compare to the case when Lambda sensor is used.

The emissions characteristics of the test vehicle show that HHO gas reduced CO emissions by 23.07% and HC emissions by 6%. However, without the lambda sensor, HHO gas increases the HC emissions by 2.45% and $CO_2$ emissions by 2.03%.

A high level increase in the emissions rate of $NO_x$ was observed with and without HHO gas when the lambda sensor is removed. This is because the formation NOx by hydrocarbon combustion occurs above 2800 F (1538 C). In vehicle system, the engine combustion temperature is kept below 1538 C by maintaining slightly rich burn condition through the lambda sensor and ECU. Therefore, when lambda sensor is removed, the combustion temperature increases more than that with lambda sensor resulting in observation of NOx formation. The $NO_x$ gas emission also increases when HHO gas is used as compared to emission without HHO gas by 7.75%.

**List of Figures**
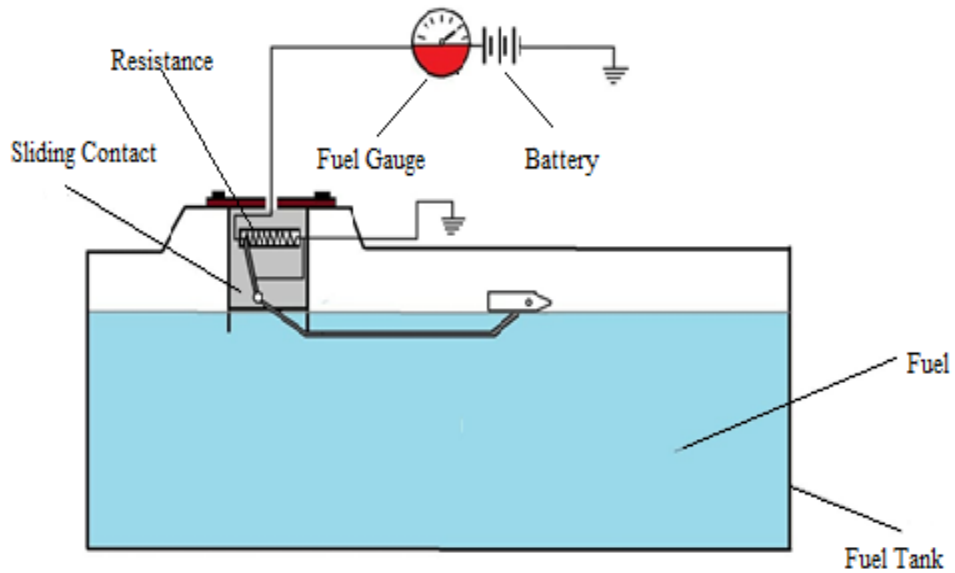


**Figure 4.1**: Block Diagram of Fuel Sending Unit
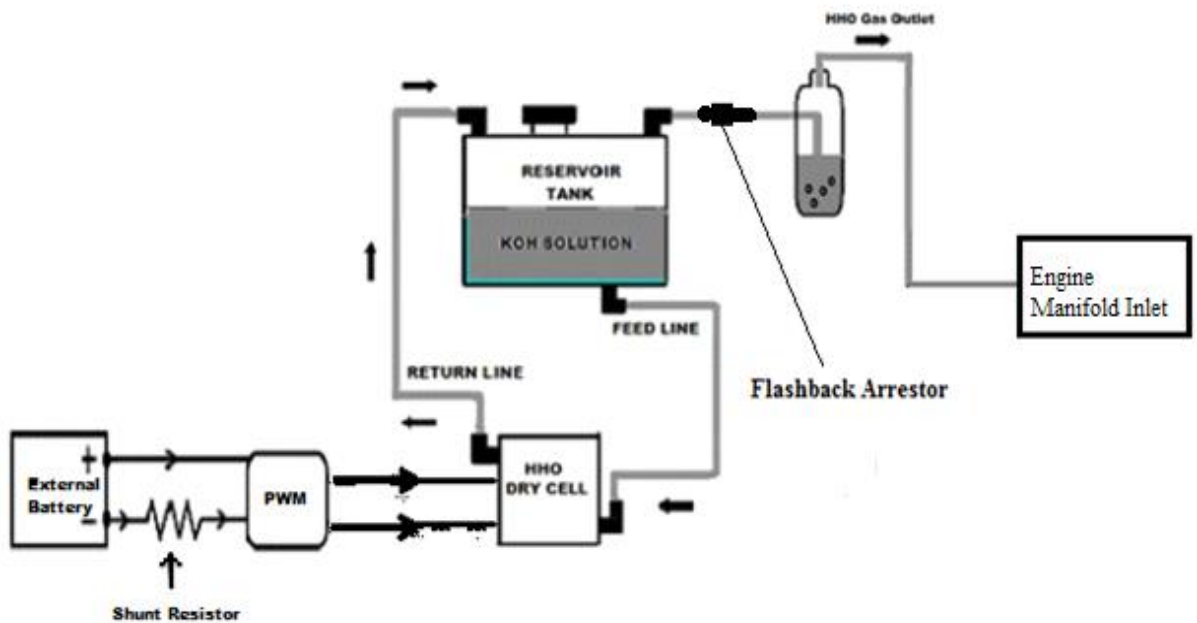


**Figure 4.2**: HHO Gas Application to The test vehicle Engine via On-board

Generating System
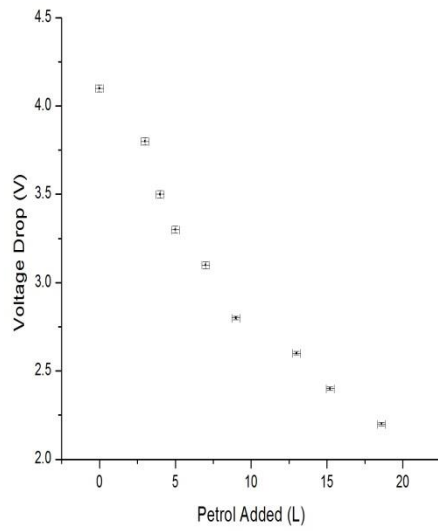
(a)
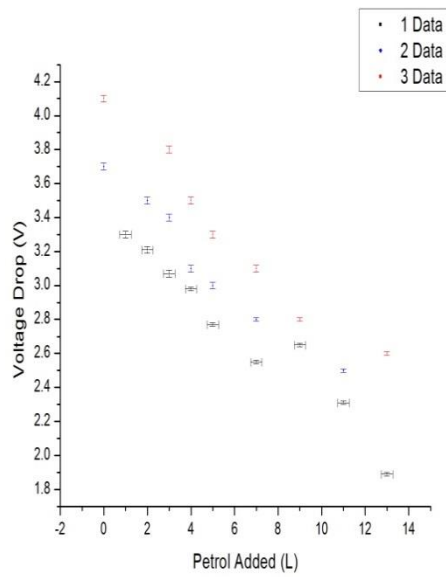


(b)

**Figure 4.3:** (a) Variation of Voltage drop for every litre of petrol addition to the Fuel

Tank

(b) Linear region of Voltage Drop Method
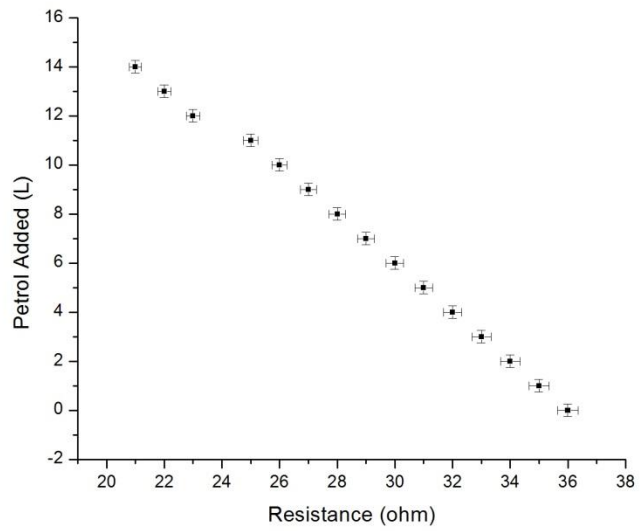
**Figure 4.4:** Variation of Resistance with fuel level in the tank
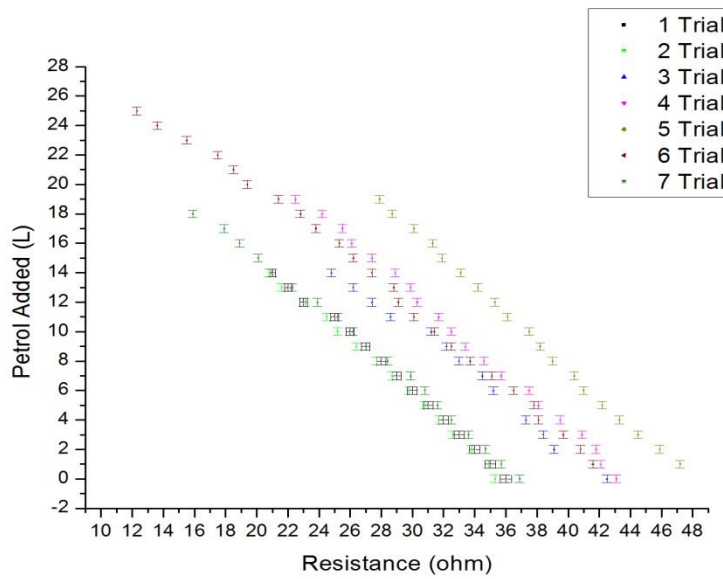


**Figure 4.5:** Resistance vs Petrol Addition (a) ■ 1 Trial (b) ●2 Trial

(c) ▲3 Trial (d) ▼ 4 Trial (e) ◄5 Trial (f) ► 6 Trial (g) ♦7 Trial
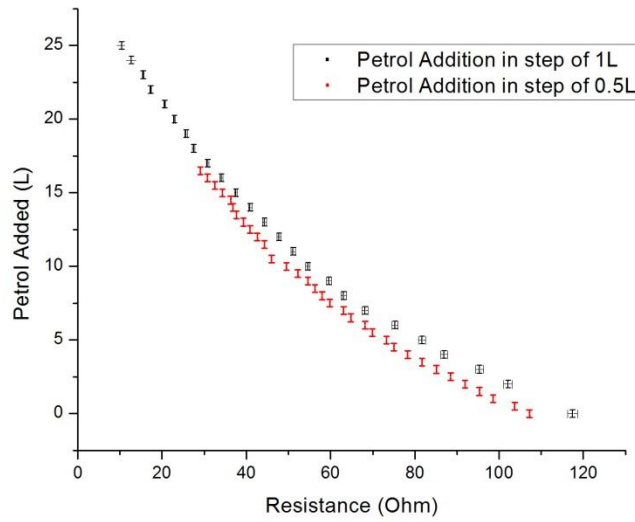
**Figure 4.6:** Resistance vs Petrol Addition of the whole fuel tank
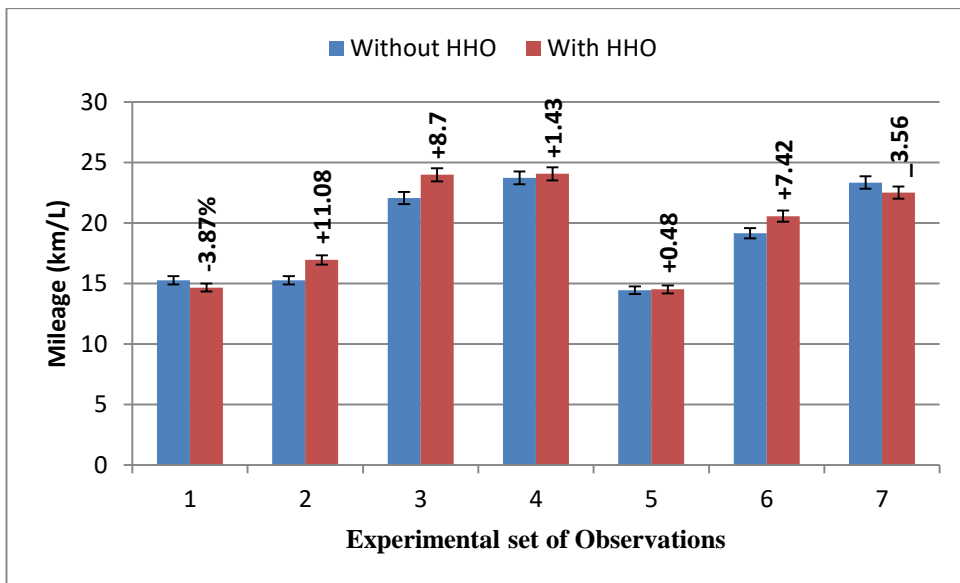


**Figure 4.7:** Effect of HHO Gas on Mileage of the test vehicle with the lambda

sensor
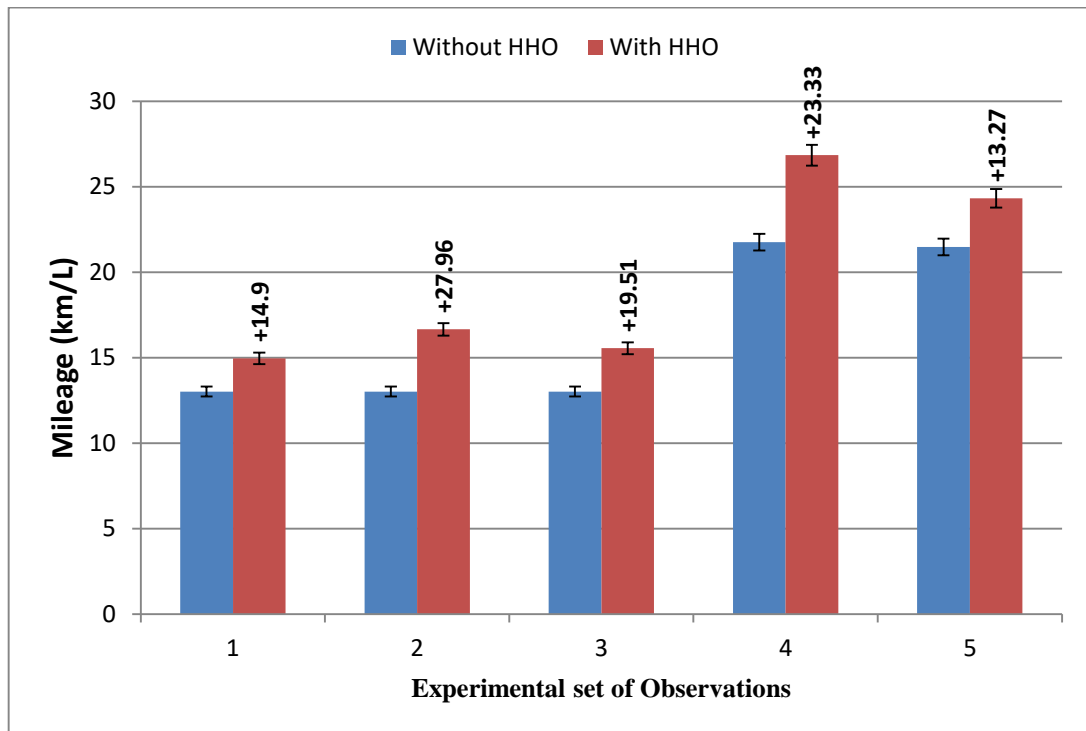
**Figure 4.8:** Effect of HHO Gas on Mileage of the test vehicle without the lambda

sensor
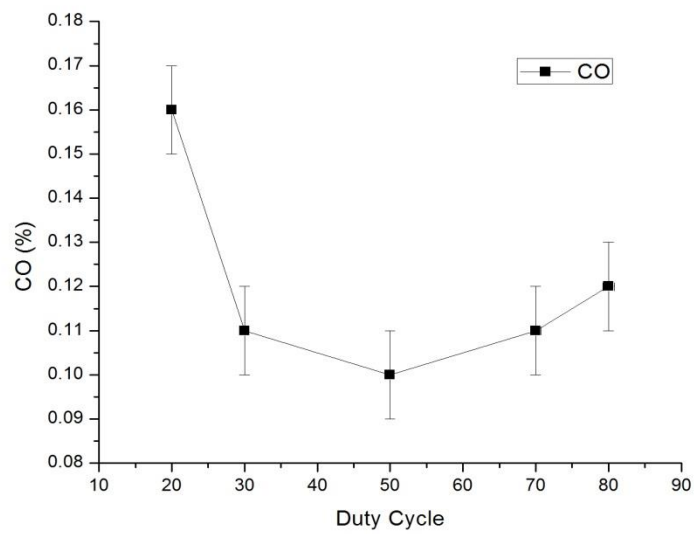


(a)
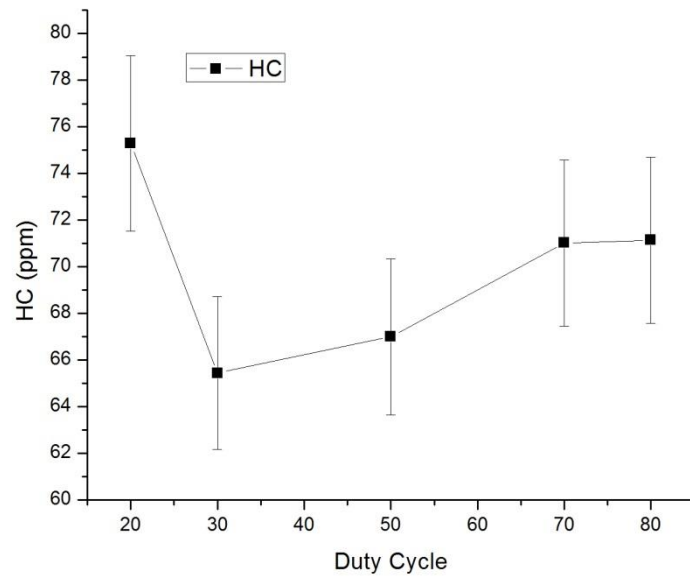
(b)
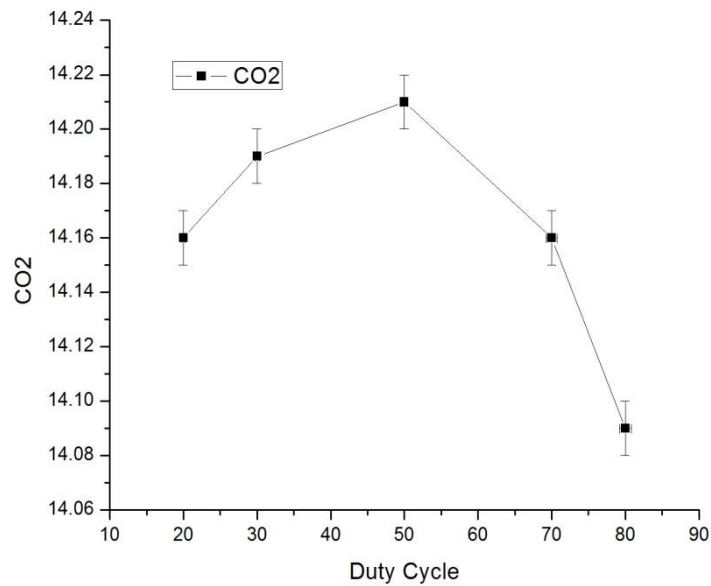


(c)

**Figure 4.9:** Variation of Tailpipe Emission with Duty Cycle (a) for Carbon monoxide (b) for Hydrocarbon (c) for carbon dioxide
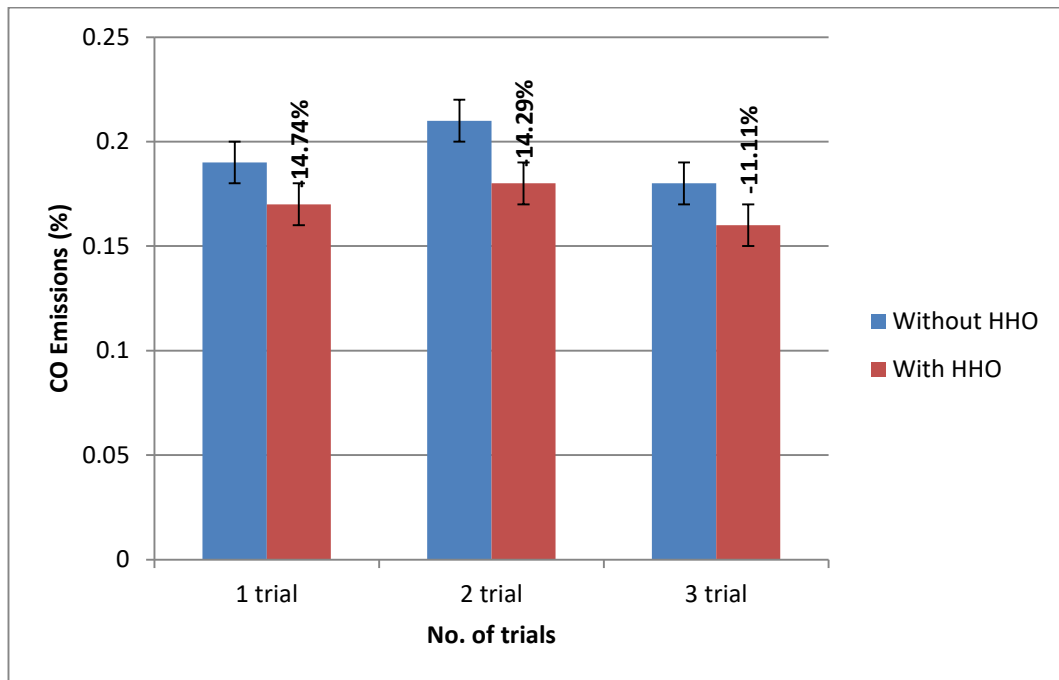
**Figure 4.10:** Effect of HHO gas on CO emissions
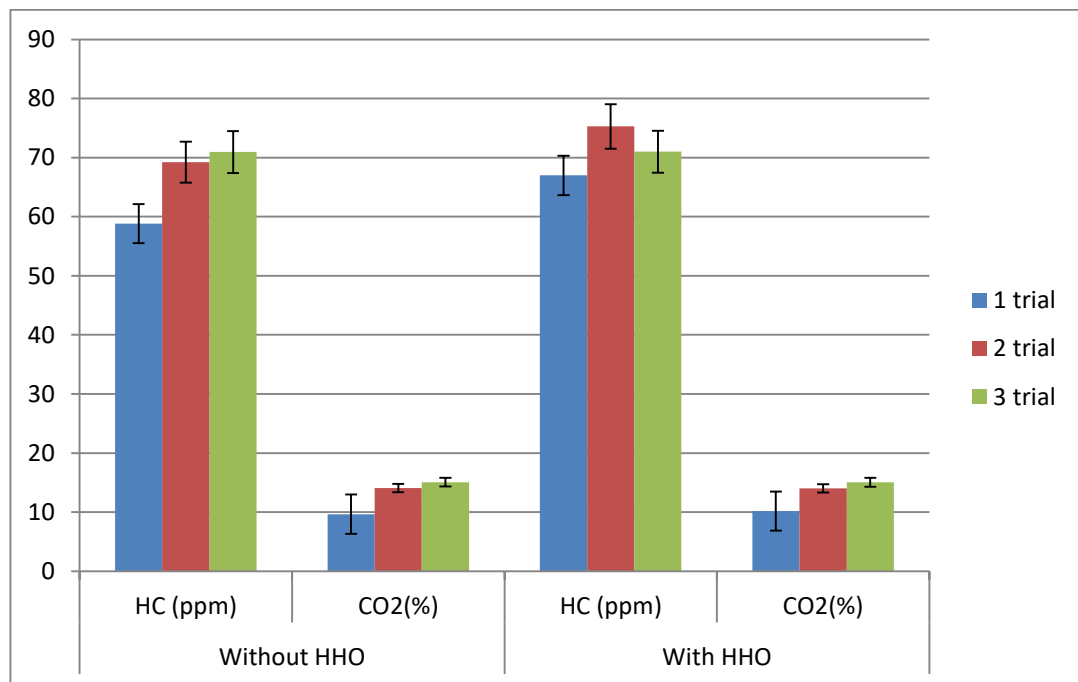


**Figure 4.11:** Effect of HHO gas on HC and $CO_2$ emissions characteristics of the test
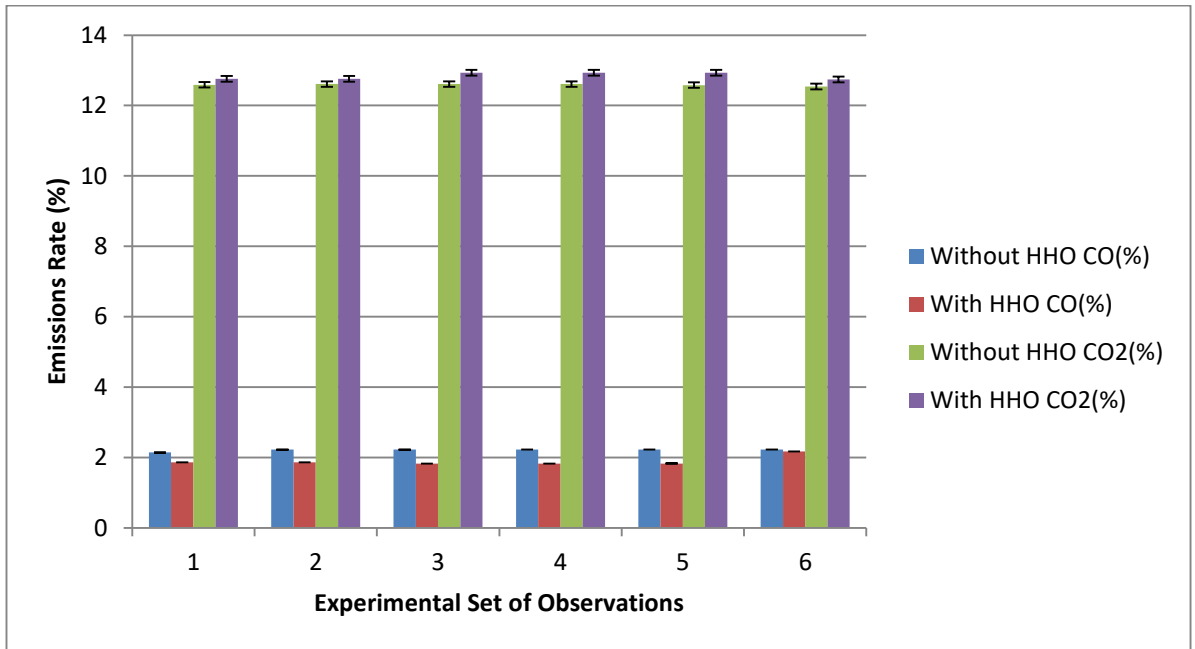
vehicle

**Figure 4.12:** Effect of HHO gas on CO and $CO_2$ emissions characteristics of the test

vehicle without the lambda sensor
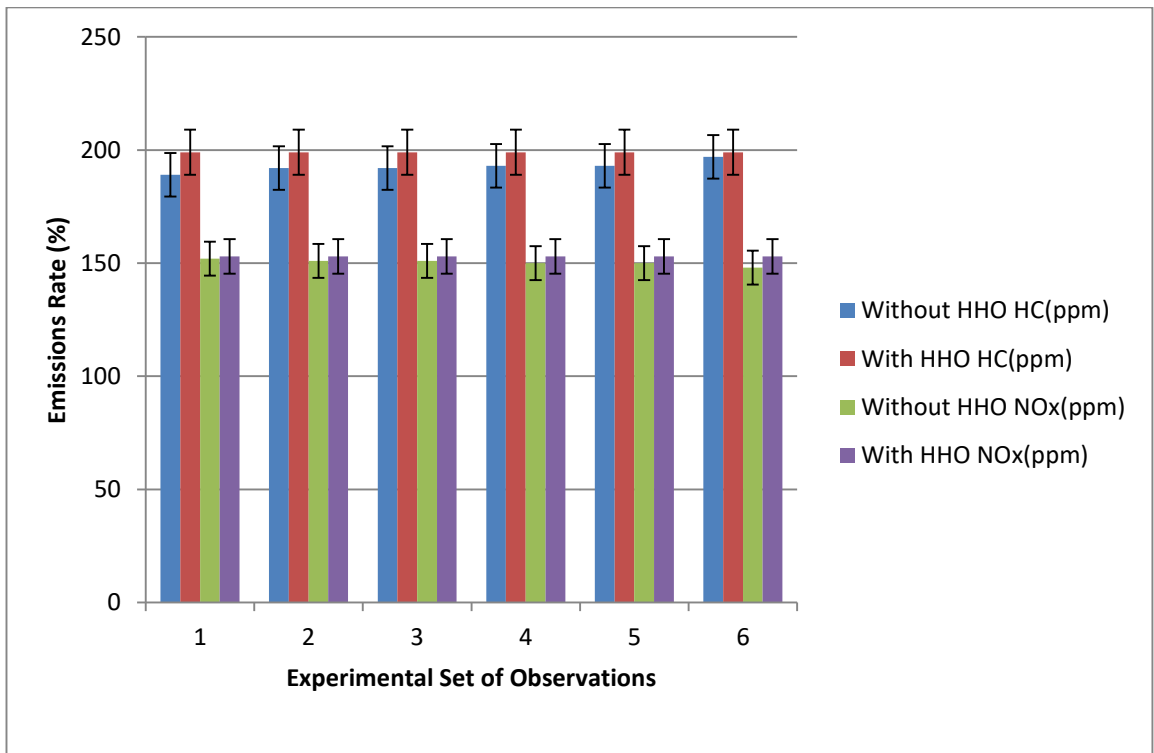


**Figure 4.13:** Effect of HHO gas on HC and $NO_x$ emissions characteristics of the test

vehicle without the lambda sensor

**List of Tables**

| Table 4.1: Variation of Voltage Drop with Petrol Addition | | | | | | | |
|---|---|---|---|---|---|---|---|
| Petrol Added | | Voltage Drop | | Voltage Drop | | Voltage Drop | |
| L | Error(±) | V | | V | | V | |
| | | 1 Data | Error(±) | 2 Data | Error(±) | 3 Data | Error(±) |
| 0 | 0.26 | 3.4 | 0.02 | 3.7 | 0.02 | 4.1 | 0.02 |
| 1 | 0.26 | 3.3 | 0.02 | -- | | -- | |
| 2 | 0.26 | 3.21 | 0.02 | 3.5 | 0.02 | -- | |
| 3 | 0.26 | 3.07 | 0.02 | 3.4 | 0.02 | 3.8 | 0.02 |
| 4 | 0.26 | 2.98 | 0.01 | 3.1 | 0.02 | 3.5 | 0.02 |
| 5 | 0.26 | 2.77 | 0.01 | 3 | 0.02 | 3.3 | 0.02 |
| 7 | 0.26 | 2.55 | 0.01 | 2.8 | 0.01 | 3.1 | 0.02 |
| 9 | 0.26 | 2.65 | 0.01 | -- | | 2.8 | 0.01 |
| 11 | 0.26 | 2.31 | 0.01 | 2.5 | 0.01 | -- | |
| 13 | 0.26 | 1.89 | 0.01 | -- | | 2.6 | 0.01 |
| 15 | 0.26 | 1.72 | 0.01 | -- | | -- | |
| 15.2 | 0.26 | -- | | 2 | 0.01 | 2.4 | 0.01 |
| 17 | 0.26 | 0.59 | 0.002 | -- | | -- | 0.01 |
| 18.6 | 0.26 | -- | | 1 | 0.01 | 2.2 | 0.01 |
| 18.7 | 0.26 | -- | | -- | | 2.1 | |

| Table 4.2: Variation of Resistance with Addition of Petrol in Linear Resistance Method | | | | | | | | |
|---|---|---|---|---|---|---|---|---|
| Petrol Added | | Resistance (Uncertainty is 1% of the rdg) | | | | | | |
| (L) | Error(±) | Ohm | | | | | | |
| | | 1 Trial | 2 Trial | 3 Trial | 4 Trial | 5 Trial | 6 Trial | 7 Trial |
| 0 | 0.26 | 36 | 35.3 | 42.5 | 43.1 | -- | -- | 36.9 |
| 1 | 0.26 | 35 | 34.9 | 41.6 | 42.1 | 47.2 | 41.6 | 35.7 |
| 2 | 0.26 | 34 | 33.8 | 39.1 | 41.8 | 45.9 | 40.8 | 34.7 |
| 3 | 0.26 | 33 | 32.6 | 38.4 | 40.9 | 44.5 | 39.7 | 33.6 |
| 4 | 0.26 | 32 | 31.7 | 37.3 | 39.5 | 43.3 | 38.1 | 32.5 |
| 5 | 0.26 | 31 | 30.8 | -- | 38.1 | 42.2 | 37.8 | 31.6 |
| 6 | 0.26 | 30 | 29.8 | 35.2 | 37.5 | 41 | 36.5 | 30.8 |

| 7 | 0.26 | 29 | 28.7 | 34.5 | 35.7 | 40.4 | 35.1 | 29.9 |
|---|------|----|------|------|------|------|------|------|
| 8 | 0.26 | 28 | 27.7 | 33 | 34.6 | 39 | 33.7 | 28.4 |
| 9 | 0.26 | 27 | 26.4 | 32.2 | 33.4 | 38.2 | 32.5 | 27 |
| 10 | 0.26 | 26 | 25.2 | 31.2 | 32.5 | 37.5 | 31.4 | 26.2 |
| 11 | 0.26 | 25 | 24.5 | 28.6 | 31.7 | 36.1 | 30.1 | 25.2 |
| 12 | 0.26 | 23 | 23.1 | 27.4 | 30.3 | 35.3 | 29.1 | 23.9 |
| 13 | 0.26 | 22 | 21.6 | 26.2 | 29.9 | 34.2 | 28.8 | 22.3 |
| 14 | 0.26 | 21 | 20.8 | 24.8 | 28.9 | 33.1 | 27.4 | 20.9 |
| 15 | 0.26 | | | | 27.4 | 31.9 | 26.2 | 20.1 |
| 16 | 0.26 | | | | 26.1 | 31.3 | 25.3 | 18.9 |
| 17 | 0.26 | | | | 25.5 | 30.1 | 23.8 | 17.9 |
| 18 | 0.26 | | | | 24.2 | 28.7 | 22.8 | 15.9 |
| 19 | 0.26 | | | | 22.5 | 27.9 | 21.4 | |
| 20 | 0.26 | | | | | | 19.4 | |
| 21 | 0.26 | | | | | | 18.5 | |
| 22 | 0.26 | | | | | | 17.5 | |
| 23 | 0.26 | | | | | | 15.5 | |
| 24 | 0.26 | | | | | | 13.6 | |
| 25 | 0.26 | | | | | | 12.3 | |
| 26 | 0.26 | | | | | | 11 | |

| Table 4.3: Linear fitting value of Resistance vs Petrol Addition | | | | |
|------------------|-------------------|-------------------|----------------|----------------|
| Observation | Intercept Value | Intercept Error | Slope Value | Slope Error |
| 1 Trial | 33.96 | 0.47 | -0.94 | 0.02 |
| 2 Trial | 33.69 | 0.43 | -0.94 | 0.02 |
| 3 Trial | 34.43 | 0.78 | -0.81 | 0.02 |
| 4 Trial | 40.18 | 0.41 | -0.92 | 0.01 |
| 5 Trial | 44.61 | 0.37 | -0.96 | 0.01 |
| 6 Trial | 36.03 | 0.34 | -0.83 | 0.01 |
| 7 Trial | 32.56 | 0.33 | -0.87 | 0.01 |
| **Average** | **36.49** | **0.45** | **-0.89** | **0.01** |

| No. of Obs | Distance travelled | | Change in Resistance(X) | Fuel Consumed (*l*) | | Mileage | |
|---|---|---|---|---|---|---|---|
| | (km) | Error(±) | | X/Slope | Error(±) | (km/L) | Error(±) |
| 1 | 12.6 | 0.2 | 1.1 | 1.24 | 0.01 | 10.19 | 0.2 |
| 2 | 18.89 | 0.2 | 1.3 | 1.46 | 0.01 | 12.93 | 0.2 |
| 3 | 18.7 | 0.2 | 1.2 | 1.35 | 0.01 | 13.86 | 0.2 |
| 4 | 18.7 | 0.2 | 1.1 | 1.24 | 0.01 | 15.13 | 0.2 |
| 5 | 18.8 | 0.2 | 1 | 1.12 | 0.01 | 16.73 | 0.2 |
| 6 | 18.8 | 0.2 | 0.9 | 1.01 | 0.01 | 18.59 | 0.2 |
| **Average** | **17.75** | | **1.1** | **1.24** | | **14.58** | |

**Table 4.4:** Mileage Measurement in Linear Resistance Method

| Petrol Added | | Resistance (in Ohm) | | | |
|---|---|---|---|---|---|
| L | Error(±) | 0.5L Addition | Error(±) | 1L Addition | Error(±) |
| 0 | 0.26 | 107.2 | 1.07 | 117.4 | 1.17 |
| 0.5 | 0.26 | 103.7 | 1.04 | -- | |
| 1 | 0.26 | 98.6 | 0.99 | -- | |
| 1.5 | 0.26 | 95.3 | 0.95 | -- | |
| 2 | 0.26 | 91.9 | 0.92 | 102.1 | 1.02 |
| 2.5 | 0.26 | 88.5 | 0.89 | -- | |
| 3 | 0.26 | 85.1 | 0.85 | 95.3 | 0.95 |
| 3.5 | 0.26 | 81.7 | 0.82 | | |
| 4 | 0.26 | 78.3 | 0.78 | 86.9 | 0.87 |
| 4.5 | 0.26 | 75 | 0.75 | | |
| 5 | 0.26 | 73.3 | 0.73 | 81.7 | 0.82 |
| 5.5 | 0.26 | 69.9 | 0.69 | | |
| 6 | 0.26 | 68.2 | 0.68 | 75.3 | 0.75 |
| 6.5 | 0.26 | 64.8 | 0.65 | | |
| 7 | 0.26 | 63.1 | 0.63 | 68.2 | 0.68 |
| 7.5 | 0.26 | 59.8 | 0.59 | | |
| 8 | 0.26 | 58 | 0.58 | 63.1 | 0.63 |
| 8.5 | 0.26 | 56.3 | 0.56 | | |
| 9 | 0.26 | 54.6 | 0.55 | 59.6 | 0.59 |
| 9.5 | 0.26 | 52.2 | 0.52 | | |
| 10 | 0.26 | 49.5 | 0.49 | 54.6 | 0.55 |

**Table 4.5:** Variation of Resistance with Addition of Petrol in Polynomial Resistance Method

| | | | | | |
|------|------|------|------|------|-------|
| 10.5 | 0.26 | 46   | 0.46 |      |       |
| 11   | 0.26 | 44.3 | 0.44 | 51.1 | 0.511 |
| 11.5 | 0.26 | 42.6 | 0.43 |      |       |
| 12   | 0.26 | 40.9 | 0.41 | 47.7 | 0.48  |
| 12.5 | 0.26 | 39.3 | 0.39 |      |       |
| 13   | 0.26 | 37.6 | 0.38 | 44.3 | 0.44  |
| 13.5 |      | 36.8 | 0.37 |      |       |
| 14   |      | 36.3 | 0.36 | 40.9 | 0.41  |
| 14.5 |      | 34.3 | 0.34 |      |       |
| 15   |      | 32.5 | 0.33 | 37.5 | 0.38  |
| 15.5 |      | 30.8 | 0.31 |      |       |
| 16   |      | 29.1 | 0.29 | 34.1 | 0.34  |
| 16.5 |      |      |      |      |       |
| 17   |      |      |      | 30.8 | 0.31  |
| 17.5 |      |      |      |      |       |
| 18   |      |      |      | 27.5 | 0.28  |
| 18.5 |      |      |      |      |       |
| 19   |      |      |      | 25.7 | 0.26  |
| 19.5 |      |      |      |      |       |
| 20   |      |      |      | 22.9 | 0.23  |
| 20.5 |      |      |      |      |       |
| 21   |      |      |      | 20.6 | 0.21  |
| 21.5 |      |      |      |      |       |
| 22   |      |      |      | 17.3 | 0.17  |
| 22.5 |      |      |      |      |       |
| 23   |      |      |      | 15.5 | 0.16  |
| 23.5 |      |      |      |      |       |
| 24   |      |      |      | 12.7 | 0.13  |
| 24.5 |      |      |      |      |       |
| 25   |      |      |      | 10.4 | 0.1   |
| 25.5 |      |      |      |      |       |
| 26   |      |      |      | 10.4 | 0.1   |

| Table 4.6: Polynomial fitting value of Resistance vs Petrol Addition | | | | | | |
|---|---|---|---|---|---|---|
| | Intercept | Intercept | B1 | B1 | B2 | B2 |
| Observations | Value | Error | Value | Error | Value | Error |
| Addition in 0.5 L | 27.59 | 0.26 | -0.42 | 0.01 | 0.002 | 6.53E-05 |
| Addition in 1 L | 29.08 | 0.19 | -0.42 | 0.01 | 0.002 | 6.31E-05 |
| **Average** | **28.34** | **0.23** | **-0.42** | **0.01** | **0.002** | **6.42E-05** |

| Table 4.7: Effect of HHO on mileage measurement of the test vehicle | | | | | | | | | | |
|---|---|---|---|---|---|---|---|---|---|---|
| No. of obs | R1- R2 | R1+ R2 | Distance travelled | Condition | $O_2$ Sensor | Speed (km/hr) | $l = L2-L1$ | Mileage | Uncertainty in Mileage | Gain/ Loss % in Mileage | |
| 1. | 2.8 | 104.2 | 10.1 | woHHO | With lambda sensor | 25-30 | 0.66 | 15.26 | 0.31 | | |
| 2. | 3.1 | 112.3 | 10.1 | HHO | | | 0.69 | 14.67 | 0.29 | L | -3.87 |
| 3. | 2.9 | 121.7 | 10.1 | HHO | | | 0.6 | 16.95 | 0.34 | G | 11.08 |
| 4. | 1.7 | 85.7 | 10.1 | woHHO | | | 0.46 | 22.07 | 0.44 | | |
| 5. | 1.7 | 99.3 | 10 | HHO | | | 0.42 | 23.99 | 0.48 | G | 8.7 |
| 6. | 1.6 | 89 | 10 | woHHO | | | 0.42 | 23.73 | 0.47 | | |
| 7. | 1.6 | 91.1 | 10 | HHO | | | 0.42 | 24.07 | 0.48 | G | 1.43 |
| 8. | 3 | 122.4 | 10 | woHHO | | | 0.61 | 14.45 | 0.29 | | |
| 9. | 3.4 | 122.2 | 10.1 | HHO | | | 0.7 | 14.52 | 0.29 | G | 0.48 |
| 10. | 1.7 | 116.3 | 7 | woHHO | | | 0.37 | 19.15 | 0.38 | | |
| 11. | 1.7 | 126.3 | 6.9 | HHO | | | 0.34 | 20.57 | 0.41 | G | 7.42 |
| 12. | 1.5 | 126.5 | 6.9 | woHHO | | | 0.3 | 23.35 | 0.47 | | |
| 13. | 1.6 | 129.6 | 6.9 | HHO | | | 0.31 | 22.52 | 0.45 | L | -3.56 |
| 14. | 5.7 | 160.9 | 10.1 | woHHO | Without lambda sensor | 25-30 | 0.78 | 13.02 | 0.26 | | |
| 15. | 4.1 | 145.7 | 10 | HHO | | | 0.69 | 14.96 | 0.29 | G | 14.9 |
| 16. | 2.9 | 119.7 | 10.1 | HHO | | | | 16.66 | 0.33 | G | 27.96 |
| 17. | 3.1 | 119.5 | 10.1 | HHO | | | 0.65 | 15.56 | 0.31 | G | 19.51 |
| 18. | 2.7 | 140.7 | 10.1 | woHHO | | | 0.46 | 21.77 | 0.44 | | |
| 19. | 2.3 | 146.3 | 10 | HHO | | | 0.37 | 26.85 | 0.54 | G | 23.33 |

| 20. | 3.1 | 152.1 | 10.1 | woHHO | | | 0.47 | 21.48 | 0.43 | | |
| 21. | 2.9 | 156.9 | 10.1 | HHO | | | 0.42 | 24.33 | 0.49 | G | 13.27 |

**Table 4.8 :** Effect of 1.5M of KOH on engine Emissions at Different Duty Cycle

(Uncertainty is 5% of the rdg)

| Duty Cycle | CO | HC | NOx (ppm) | $O_2$ | $CO_2$ |
|---|---|---|---|---|---|
| % | % | ppm | | % | % |
| 20 | 0.16 | 75.29 | 0 | 0.43 | 14.16 |
| 30 | 0.11 | 65.44 | 0 | 0.43 | 14.19 |
| 50 | 0.1 | 67 | 0 | 0.39 | 14.21 |
| 70 | 0.11 | 71.02 | 0 | 0.39 | 14.16 |
| 80 | 0.12 | 71.15 | 0 | 0.359 | 14.09 |

**Table 4.9:** Effect of HHO gas on emissions of the test vehicle
(Uncertainty is 5% of the rdg)

| No. of Trials | Without HHO | | | With HHO | | |
|---|---|---|---|---|---|---|
| | CO | HC | $CO_2$ | CO | HC | $CO_2$ |
| | % | ppm | % | % | ppm | % |
| 1 trial | 0.19 | 58.84 | 9.64 | 0.16 | 67 | 10.17 |
| 2 trial | 0.21 | 69.23 | 14.05 | 0.18 | 75.29 | 14.03 |
| 3 trial | 0.18 | 70.95 | 15.07 | 0.16 | 71.02 | 15.05 |

**Table 4.10:** Effect of HHO gas on emissions of Test Vehicle without Lambda sensor
(Uncertainty is 5% of the rdg)

| Without HHO | | | | With HHO | | | |
|---|---|---|---|---|---|---|---|
| CO (%) | $CO_2$ (%) | HC (ppm) | NOx (ppm) | CO (%) | $CO_2$ (%) | HC (ppm) | NOx (ppm) |
| 2.14 | 12.59 | 189 | 152 | 1.86 | 12.76 | 199 | 153 |
| 2.23 | 12.61 | 192 | 151 | 1.863 | 12.76 | 199 | 153 |
| 2.23 | 12.61 | 192 | 151 | 1.83 | 12.93 | 199 | 153 |
| 2.23 | 12.61 | 193 | 150 | 1.83 | 12.93 | 199 | 153 |
| 2.23 | 12.58 | 193 | 150 | 1.83 | 12.93 | 199 | 153 |
| 2.23 | 12.54 | 197 | 148 | 2.17 | 12.74 | 199 | 153 |

# CHAPTER 5

# SUMMARY AND CONCLUSIONS

## 5. SUMMARY AND CONCLUSIONS

In this Ph.D research work, the application of hydrogen gas in a form called Brown's gas or HHO gas as fuel additive to a hydrocarbon fuel namely gasoline or petrol was studied. The work covers both the hydrogen gas production and the application parts. Hydroxy gas is produced by alkaline water electrolysis with KOH as electrolyte in an 11-plates common-ducted HHO dry cell. The dependence of HHO gas production rate on concentration, temperature, current, duty cycle and cell voltage was investigated in Chapter 3. The observed variations of HHO production rate with the all the above mentioned parameters could be explained based on the variation of the electrolyte specific conductivity with temperature and concentration. Due to the variation of electrolyte conductivity with temperature, HHO gas production rate is found to be linearly dependent on temperature. The electric power consumed also follows the same pattern while the voltage remained constant at around 11.5 V. Within the concentration range of 1 M to 5 M, the association of ions at higher concentration caused the gas flow rate to first increases linearly with the concentration and then decrease. Similarly, the increase in concentration of ions causes more current to flow through the solution, and hence the electric power consumed increased. The maximum point for flowrate and power appear to occur between 3 and 4 M KOH concentration. At a given concentration of KOH, the HHO production increases with increase in the duty cycle. The electrolysis characteristics at 1 M and 2 M shows that the voltage and hence the current required for 2 M concentrations is a bit lower as compared to 1 M. This is because of the presence of larger number of free electrons at higher concentration to increase the conductivity.

*Summary & Conclusions*

The increase in the specific conductivity results in lower current consumption for electrolysis. According to 1/2 or 1/4 rule, a 2 M KOH electrolyte solution that can produce a maximum of 1.38 ± 10% LPM of HHO gas with power consumption of 175.6 Watt and 50.40 Celsius temperature was sufficient enough for the concerned research work. At this point the current consumed by the whole electrolyzer unit was measured to be 14.63 A at 12 V. The cell potential or cell voltage is 2.4 V which is above the thermoneutral voltage of 1.48 V. As the cell voltage used in this experiment was larger than the thermoneutral voltage, the temperature of the solution also increases during electrolysis process which further affects the hydrogen production rate. The electrical efficiency of the electrolyzer is estimated to be 61.67 % at 175.6 Watt. The deviation of the efficiency from ideal electrolysis efficiency can be attributed to the various energy losses: electrical loss due to wiring and ions, transport losses due to formation of bubbles and resistances formed by ions, and energy loss due to hydrogen evolution reaction (HER) and oxygen evolution reaction (OER).

The electrolyzer was powered by the lead accumulator of 48 AH and the alternator of the test vehicle. The maximum current that can be drawn from the engine alternator is 35 A. The amount of current required for the working of the fuel pump in the concerned vehicle is 16 A. The headlight alone consumed 12.53 A, ignition required 0.93 A, 2.66 A for the indicator and breaklight used 4.13 A. Out of the alternator rating of 35 A, the minimum amount of amperage required to be reserved for all the electrical components of the vehicle is estimated to 25 A at 12 V and only about 10 A is available for the electrolyzer. These observations suggested that onboard generation of HHO gas using 11-plates HHO dry cell is feasible if the

requirement of HHO gas flowrate is below 0.8 LPM. Above this limit and upto 1.38 LPM requirement of HHO gas, only daytime driving where the headlight is switch OFF is recommended.

In Chapter 4, the experimental results of HHO gas introduction as fuel supplement were presented and discussed. Understanding the effect of Brown's gas on the mileage performance of Maruti 800 required a complete accurate measurement of the fuel consumption rate of the vehicle. The fuel consumption rate measurement through the fuel gauge was neglected in favour of measurement by calibration of the fuel tank. In this research work, three methods were tried for the accurate measurement of fuel consumption rate namely: The Voltage Drop Method, The Linear Resistance Method (LRM) and The Polynomial Resistance Method (PRM). In the three methods, the fuel (petrol) is added in step of 1 L and the corresponding voltage/resistance is recorded. However, in voltage drop method, the low battery voltage towards the end of each experiment prevents us from getting an accurate value in measuring the fuel consumption rate. Thus, the Linear Resistance Method was developed. The resistance value drop as petrol was added to the fuel tank. A graph of the resistance recorded was plotted with the petrol added. Linear fitting of the recorded data shows that the average slope of the linear fit was about 0.89 L/R. However, as a result of the connection between the fuel gauge and fuel sender unit, the fuel that went back to the fuel tank through the return line cause the temperature of the petrol inside the fuel tank to increase. A minimum of around 30 minutes was required to cool down the temperature of the petrol before each reading was recorded. This makes it impossible to obtained instantaneous data through the

Linear Resistance Method and was neglected in favor of The Polynomial Resistance Method.

In Polynomial Resistance Method (PRM), the connection between fuel gauge and fuel sender unit is terminated. Experimental data can be recorded instantaneously with each addition of petrol. The polynomial plot of the fuel consumption rate to the resistance is used for calculating the mileage of Maruti 800. It was found that with polynomial fitting; even a change of 0.5 L of fuel can be measured. The uncertainty in mileage measurement using this method was estimated to be within 10%. The average mileages obtained for the test vehicle in a traffic free road conditions were around 14.58 and 18.86 km/L at the speed of 25-30 km/hr according to LRM and PRM.

In mileage measurement, out of 7 test runs for 10.1 km at the speed of 25-30 km/hr, the 6 test shows mileage improvement while 2 tests is negative. That means 71 % success rate. The highest mileage gain achieved was 27.96% and is observed when the lambda sensor is removed while the highest mileage gain with to lambda sensor is 11.08%. Thus, the mileage gain when the lambda sensor is removed is 14.04% higher than mileage gain under normal condition. This can be attributed to the fact that the removal of the lambda sensor caused the engine to acts as carburetor type of engine and the engine no longer has to maintain a stoichiometric air-fuel ratio of 14.7:1. The overall increase in mileage with the supplement of hydrogen gas was found to be 13.31%.

At 100% duty cycle of 2 M KOH concentration and 1.38 LPM HHO flowrate, CO emission showed improvement by 13.38 % while HC emission was observed to increase by 7.57%. As a result of the conversion of CO to $CO_2$, the emission

characteristic of $CO_2$ is inversely proportional to that of CO emission. The increased in $CO_2$ emissions confirmed the occurrence of better engine combustion in the presence of HHO gas as fuel supplement. However, HHO gas increases the HC emissions by 2.45% and $CO_2$ emissions by 2.03% without the lambda sensor. A high level increase in the emissions rate of NOx was observed with and without HHO gas when the lambda sensor is removed. The NOx gas emission also increases when HHO gas is used as compared to emission without HHO gas by 7.75%.

Overall, electrolysis of water to produce hydrogen may prove beneficial for transport and other industrial purposes, leaning towards clean environment and reduction in global warming. In terms of fuel requirements of current global trends, hydrogen rich gas as fuel supplement in internal combustion engine seems a possible solution in meeting the daily demands. Hydroxy gas fuel supplement looks like a perfect choice for the future.

**Future Scope of Study**

From the results of this whole work and the present stage of our understanding, the following future work plans are proposed

a) Further improvement in the electrolyzer efficiency of HHO gas generation is required which will also open a way for fossil fuel replacement by hydrogen. Two techniques are proposed – High frequency pulse electrolysis and high temperature water electrolysis.

b) Petrol engine emission levels are much lower compare diesel engine and therefore it will be more needful to apply the technique to diesel powered vehicle.

# REFERENCES

# REFERENCES

Abdel-Rahman AA, (1998), On the emissions from internal-combustion engines: A review, *Int J Energy Res*, **22(6)**, 483–513.

A.C.Yilmaz, Uludamar E. E. and Aydin K., (2010), Effect of hydroxy (HHO) gas addition on performance and exhaust emissions in compression ignition engines, *Int. J. Hydrogen Energy*, **vol. 35**, 11366-11372.

Ali Kilicarslana and Mohamad Qatu, (2017), Exhaust gas analysis of an eight cylinder gasoline engine based on engine speed, 1st International Conference on Energy and Power, ICEP2016, 14-16 December 2016, RMIT University, Melbourne, Australia, *Energy Procedia*, **110 ,** 459 – 464.

Andrea T.D., Henshaw P.F., Ting D.S.K., (2004), The addition of hydrogen to a gasoline – fuelled SI engine, *International Journal of Hydrogen Energy*, **29**, 1541–52.

Anh T.L., Duc K.N., Thu H.T.T., Van T.C., (2013), Improving Performance and Reducing Pollution Emissions of a Carburetor Gasoline Engine by Adding HHO Gas into the Intake Manifold, *SAE International*, 2013-01-0104.

Antunes G.J.M, Mikalsen R., Roskilly A.P., (2009), An experimental study of a direct injection compression ignition hydrogen engine, *International Journal of Hydrogen Energy,***34**: 6516- 6522.

## *References*

Arat H.T., Baltacioglu M.K., Ozcanli M., Aydin K (2015), Effect of using Hydroxy - CNG fuel mixtures in a non-modified diesel engine by substitution of diesel fuel, *Int J Hydrogen Energy*,1-10.

Bahng G.W., Jang D., Kim Y., Shin M., (2016), A new technology to overcome the limits of HCCI engine through fuel modification, *Appl. Therm Eng*, **98**:810-5.

Balat M., (2008), Potential importance of hydrogen as a future solution to environmental and transportation problems, *Int J Hydrog Energy*, **33**, 4013–29.

Baltacioglu M. K., Arat H.T., Baltacioglu M.K., Ozcanli M., Aydin K (2016), Experimental comparison of pure hydrogen and HHO (hydroxy) enriched biodiesel (B10) fuel in a commercial diesel engine, Int J Hydrogen Energy, 41,8347-53.

Bari S. & Mohammad E.M., (2010), Effect of H2/O2 addition in increasing the thermal efficiency of a diesel engine, *Fuel*, **89**, 378–383.

Birtas A, Chiriac R.,(2011), A study of injection timing for a diesel engine operating with gasoil and HRG gas, *UPB Sci Bull Ser D Mech Eng* ,73.

Bockris J.O.M., Conway B.E., Yeager E. and White R.E., (1981),Comprehensive Treatise of Electrochemistry, *New York: Plenum Press*.

Calo J.M., (2007), Comments on A new gaseous and combustible form of water, by R. M. Santilli, *Int J Hydrogen Energy*, **32:1309**-12.

## References

Cardona H.I., Ortega E.,Vázquez-Gómez L., Pérez-Herranz V., (2012), Porous Ni and Ni-Co electrodeposits for alkaline water electrolysis-energy saving, *Int J Chem Mol Nuc Mat Metall Eng*, **6**:823-9.

Cassidy J.F., (1977), Emissions and total energy consumption of a multicylinder piston engine running on gasoline and a hydrogen-gasoline mixture, NASA Technical Note, NASA TN D-8487.

Ceviz M.A., Sen A.K., Küleri A.K., Öner İ.V., (2012), Engine performance, exhaust emissions, and cyclic variations in a lean-burn SI engine fueled by gasoline-hydrogen blends, *Applied Thermal Engineering*, **36**, 314-324.

D.J. Pickett, (1979), Electrochemical Reactor Design*, Elsevier Scientific Publishing Co.*, New York, 121.

De Souza R.F., Loget G., Padilha J.C., Martini E.M.A. and de Souza M.O., (2008), Molybdenum electrodes for hydrogen production by water electrolysis using ionic liquid electrolytes, *Electrochemistry Communications*, **10**, 1673-1675.

Dincer I, Acar C, (2015), Review and evaluation of hydrogen production methods for better sustainability, International Journal of Hydrogen Energy, 1-8.

Dr. N.K. Giri, (2009), Automobile Mechanical, New Delhi, Khanna Publisher, pp. 376.

Du Yaodong, Yu Xiumin, Liu Lin, Li Runzeng, Zuo Xiongyinan, Sun Yao, (2017), Effect of addition of hydrogen and exhaust gas recirculation on characteristics of hydrogen gasoline engine, Int J Hydrogen Energy, **42**,8288-98.

## References

Dulger Z. & Ozcelik K.R.,(2000), Fuel economy improvement by on board electrolytic hydrogen production, *Int J Hydrogen Energy*, **25**, 895–897.

Dunn, S. (2002), Hydrogen Futures: Toward a Sustainable Energy System, International Journal of Hydrogen Energy, 27, 235-264.

Edward T. J, Heywood John B., (2003), Lean-burn characteristics of a gasoline engine enriched with hydrogen from a plasmatron fuel reformer, SAE Technical Paper No.2003-01-0630.

Egan D.R., De León C.P., Wood R.J., Jones R.L., Stokes K.R., Walsh FC., (2013), Developments in electrode materials and electrolytes for aluminium–air batteries, *J Power Sources*, **236**:293–310.

Eric McLamb. The History of Energy Use. 9.3.2011. Accessed on 05.10.2018.

Ganesh R.H, Subramanian V., Balasubramanian V., Mallikarjuna J.M., Ramesh A., Sharma R.P., (2008), Hydrogen fuelled spark-ignition engine with electronically controlled manifold injection: an experimental study. *Renew Energ*, **33**:1324-33.

Gilliam R.J., Graydon J.W, Kirk D.W. and Thorpe S.J., (2007), A review of specific conductivities of potassium hydroxide solutions for various concentrations and temperatures, *Int J Hydrogen Energy*, **32**, 359–364.

Goyal S.K., Ghatge S.V., Nema, P., and Tamhane, S.M., (2006), Understanding Urban Vehicular Pollution Problem Vis-a-Vis Ambient Air Quality – Case Study of a Megacity (Delhi, India), *Environmental Monitoring and Assessment*, **119**, 557-569.

*References*

Granovskii M, Dincer I, Rosen MA, (2006), Environmental and economic aspects of hydrogen production and utilization in fuel cell vehicles, *J Power Sources*, **157**: 411–21.

Hoffman P., (2001), Tomorrow's energy: Hydrogen, Fuel Cells, and the prospects for a cleaner Planet, *MIT Press*, Cambridge, England.

Isao Abe, (2009), Alkaline Water Electrolysis,*Energy Carriers and Conversion Systems*, EOLSS, Eds. Tokio Ohta and Veziroglu T N. **vol-I**, pp 146–166.

i3sys User Manual, 2012.

Ji C.W., Wang S.F., (2009), Effect of hydrogen addition on combustion and emissions performance of a spark ignition gasoline engine at lean conditions, *International Journal of Hydrogen Energy*, **34**, 7823- 7834.

K. Zeng and D.Zhang, (2010), Recent progress in alkaline water electrolysis for hydrogen production and applications, *Progress in Energy and Combustion Science*, **36**, 307–326.

Kandah M.I, (2014), Enhancement of Water Electrolyzer Efficiency, *Journal of Energy Technologies and Policy*, **4**, 11.

Kaveh Mazloomi, Nasri b. Sulaiman and Moayedi H., (2012), Electrical efficiency of electrolytic hydrogen production, *Int J Electrochem Sci*, **7**, 3314–3326.

Karagöz Y., Orak E., Yüksek, L., Sandalci, T., (2015), Effect of hydrogen addition on exhaust emissions and performance of a spark ignition engine, *Environ. Eng. Manag. J.*, **14**, 665–672.

*References*

Kreuter W. and Hofmann H., (1998), Electrolysis: The Important Energy Transformer in a world of Sustainable Energy, *Int. J. Hydrogen Energy*, **vol. 23**, No. 8, pp. 661666.

LeRoy R.L., Janjua M.B.I, Renaud R. and Leuenberger U., (1979), Analysis of time variation effects in water electrolyzer, *J. Electrochem.Soc.*, **126**, 1674-1682.

Mahrous A-F.M, Sakr I.M., Balabel A. and Ibrahim K., (2011), Experimental Investigation of the operating parameters affecting hydrogen production process through alkaline water electrolysis, *Int J Thermal Environ Enging*, **2**, 113–116.

Mandal B. , Sirkar A., Abhra Shau , P. De , P. Ray, (2012), Effects of Geometry of Electrodes and Pulsating DC Input on Water Splitting for Production of Hydrogen, *International journal of renewable energy research*, **vol.2**, No.1.

Milind Y.S., Dr. Sawant S.M., (2011), Investigations on Oxy-Hydrogen Gas and Producer Gas, as Alternative Fuels, On The Performance Of Twin Cylinder Diesel Engine, *Int. J. of Mechanical Engineering and Technology*, **vol.2**, 85-98.

M. M. EL-Kassaby, Yehia A. Eldrainy, Mohamed E. Khidr, Kareem I. Khidr,(2016), Effect of hydroxy (HHO) gas addition on gasoline engine performance and emissions, *Alexandria Engineering Journal*, **55**, 243–251.

Md.S. Opu, (2015), Effect of operating parameters on performance of alkaline water Electrolysis, *Int. J. Therm. Environ. Eng*, **9**, 53–60.

*References*

Musmar S.A. and Al-Rousan A.A., (2011), Effect of HHO gas on combustion emissions in gasoline engines, *Fuel*, **vol. 90**, 3066-3070.

Nagai N., Takeuchi M., Kimura T. and Oka T., (2003), Existence of optimum space between electrodes on hydrogen production by water electrolysis, *International Journal of Hydrogen Energy*, **28**, 35-41.

Paul Brand, (2006), Chapter 4 Alternator Charging System, in How To Repair Your Car, Motorbook International, 61.

Rozdman K. Mazlan, Reduan M. Dan, Mohd Z. Zakaria and Abdul H. A. Hamid, (2017), Experimental study on the effect of alternator speed to the car charging system, *The 2nd International Conference on Automotive Innovation and Green Vehicle (AiGEV 2016)*, MATEC Web Conf., Volume 90, 2017.

Samuel S., McCormick G., (2010), Hydrogen enriched diesel Combustion, *SAE Tech Paper*, 2010-01-2190.

Santilli R.M., (2006) A new gaseous and combustible form of water, *Int J Hydrogen Energy*, **31**:1113-28.

Saravanan N., Nagarajan G., (2008), An experimental investigation of hydrogen-enriched air induction in a diesel engine system, *Int J Hydrogen Energy*, **33**,1769-1775.

Seth Dunn (2002), Hydrogen futures: toward a sustainable energy system, *International Journal of Hydrogen Energy*, **27**, 235–264.

## *References*


Sharma D., Pathak D.K., Chhikara K., (2015), Performance analysis of a four stroke multi- cylinder spark ignition engine powered by a hydroxy gas booster, *J Aeronaut Automot Eng*, **2**:11-5.

Sheehan J., Camobreco V., Duffield, J., Graboski M. & Shapouri H.,(1998), Life Cycle Inventory of Biodiesel and Petroleum Diesel for Use in an Urban Bus (Natl. Renewable Energy Lab., Golden, CO), NREL Publ. No.SR-580-24089.

Shrivastava R.K., Neeta, S. And Geeta, G., (2013), Air Pollution due to road transportation in India: A review on assessment and reduction strategies, *J. Envi. Res. Development*, **8**, 69.

Sood P.R., (2012), Air Pollution Through Vehicular Emissions in Urban India and Preventive Measures, *International Conference on Environment, Energy and Biotechnology*, IPCBEE, **33**, 45-49.

Sopena C., Diéguez P.M., Sainz D., Urroz J.C., Guelbenzu E., Gandá L.M.,( 2010), Conversion of a commercial spark ignition engine to run on hydrogen: performance comparison using hydrogen and gasoline, *Int J Hydrogen Energy*,**35(3)**, 1420–9.


Steinfeld A., (2002), Solar hydrogen production via a two-step water-splitting thermochemical cycle based on Zn/ZnO redox reactions, Int J Hydrogen Energy, **27**, 611–9.

Subramanian B., Ismail S. (2018), Production and use of HHO gas in IC Engines, *International Journal of Hydrogen Energy*, 1-15.

*References*

Suryawanshi J. G., Nitnaware P. T., (2011), Performance And Emission Reduction of Multi Cylinder Gasoline Engine Using CNG Sequential Injection, *G. J. P&A Sc and Tech.*, **1**, 36- 48.

Tamer M. Ismaila, Khaled Ramzya, M.N. Abelwhabb, Basem E. Elnaghib, M. Abd El-Salamc, M.I. Ismaild, (2018), Performance of hybrid compression ignition engine using hydroxy (HHO) from dry cell, *Energy Conversion and Management*, **155**, 287–300.

Uykur C., Henshaw P.F., Ting D.S-K, Barron R.M.,(2001), Effects of addition of electrolysis product on methane/air premixed laminar combustion, *International Journal of Hydrogen Energy*, **26**,265–73.

V. M. Nikolic, Tasic G. S., Maksic A. D., Saponjic D. P., Miulovic S. M. and Marceta Kaninski M. P., (2010), Raising efficiency of hydrogen generation from alkaline water electrolysis – energy saving, *International Journal of Hydrogen Energy*, **35**: 12369–73..

Varde, K. S., Frame, G. A., (1983), Hydrogen Aspiration in a Direct Injection Type Diesel Engine-Its Effects on Smoke and other Engine Performance Parameters, *International Journal Hydrogen Energy*, **8 (7)**, 549-555.

Wang H.K., Cheng C.Y., Lin Y.C. and Chen K.S., (2012), Emission reductions of Air Pollutants from a Heavy-duty Diesel Engine Mixed with Various Amounts of H2/O2, *Aerosol and Air Quality Research*, **12**, 133–140..

*References*

Yi H. S., Lee S. J., Kim E. S., (1995), Performance Evaluation and Emission Characteristics of in-Cylinder Injection Type Hydrogen Fueled Engine, *International Journal Hydrogen Energy*, **21 (7)**, 617-624.

Yuvaraj A.L. & Santhanaraj D., (2014), A systematic study on electrolytic production of hydrogen gas by using graphite as electrode, Mat Res, **17**, 83–87.

Z.D.Wei, Ji M.B., Chen S.G., Liu Y., Sun C.X., Yin G.Z., Chen P.K. and Chan S.H. (2007). Water electrolysis on carbon electrodes enhanced by surfactant, *Electrochim. Acta*, **52**, 3323-3329

**Research Publications**

**(A) Referred Journals**

1. **J. Lalnunthari**, Lalrolaia and H. H. Thanga (2015), Analysis of petrol quality of Aizawl for oxygenate additives by FTIR-ATR spectroscopic technique, *Science Vision*, **15(4)**, 0975-6175.

2. H.H. Thanga and **J. Lalnunthari** (2015), Application of Hydrogen as Fuel Supplement in Internal Combustion Engines-A Brief Review, *International Journal for Scientific Research & Development*, **3(10)**, 2321-0613.

3. **J. Lalnunthari** and Hranghmingthanga (2015), Characterization of a multi-electrode common-ducted HHO dry cell, *Science Vision*, **15(2)**, 0975-6175.

4. **Lalnunthari J.** and Thanga H.H. (2015), Detection of Methyl tert-butyl Ether (MTBE) in Gasoline Fuel using FTIR: ATR spectroscopy, *International Research Journal of Environment Sciences*, **4(12),** 65-68.

5. H.H. Thanga and **J. Lalnunthari** (2016), A Review on the Application of Hydrogen Rich Gas as Fuel Supplement in CI and SI Internal Combustion Engine, *Research Journal of Engineering Sciences*, International Science Congress Association, **5(1),** 1-3.

6. L. R. Hlondo, B. Lalremruata, L. R. M. Punte, L. Rebecca, **J. Lalnunthari** and H. H. Thanga, (2016), A revisit to self-excited push pull vacuum tube radio frequency oscillator for ion sources and power measurements, *Review of Scientific Instruments*, American Institute of Physics, **87**, 045101: 1-6.

**(B) Conference Proceedings**

1. **J. Lalnunthari** and H. H. Thanga (2017), Dependence of Hall effect flow sensor frequency on the attached inlet and outlet pipe size, 2$^{nd}$ International Conference on Consumer Electronics Asia (ICCE-Asia), 2018, 978-1-5386-2787-7.

**Conferences Attended**

1. 8th National Conference of the Physics Academy of North East, 17-19 August, 2012,

   Department of Physics, Aizawl, Mizoram University; *Study of Electronic and Optical*

   *properties of BeX (X= S, Se & Te).*

2. UGC-Sponsored National Level Interaction Programme for Ph.D Scholars, Academic Staff College, Aizawl, Mizoram University, Mizoram, India; 23 September – 12 October, 2013.

3. National Seminar on Management of national Resources for Sustainable Development : Challenges and Procedure, 6-7 March, 2014, Department of Geography and Resource Management, School of Earth Sciences, Mizoram University, Aizawl- 796004.

4. Inter University Accelerator Centre, New Delhi sponsored- One Day State Level Acquaintance Programme, Department of Physics, Aizawl, Mizoram University, Mizoram, India; 28th March, 2014.

5. 2nd International Conference on Consumer Electronics Asia (ICCE-Asia), 6-7 October, 2017, Bengaluru, India.

## Workshop Attended

1. National Workshop on Research Methodology in Social Science for PhD Scholars, Department of Library and Information Science, Mizoram University, Aizawl, sponsored by Indian Council of Social Science Research (ICSSR), New Delhi, 5-14 March, 2013.

2. Two Days Workshop on Physics Teaching in Higher Secondary Schools Mizoram, Department of Physics, Mizoram University,8-9 May, 2014.

3. UGC-Sponsored Short Term Course One Week Workshop on Applied Statistics, Academic Staff College, Aizawl, Mizoram University, Mizoram, India; 23-28 September, 2013.

4. Orientation Workshop on Radiation-Its Application in Chemical, Physical and Life Sciences, organized jointly by UGC-DAE Consortium for Scientific Research, Kolkata Centre and Department of Chemistry, Mizoram University, Aizawl, 29-31 October, 2014.

5. A Two Days National Workshop on Error Propagation in Nuclear Reaction Data Measurement-2017 (EPNRDM-2017), Department of Physics, Aizawl, Mizoram University, Mizoram, India; 13-14 March, 2017.

**PARTICULARS OF THE CANDIDATE**

NAME OF CANDIDATE   : J. Lalnunthari

DEGREE   : Ph.D

DEPARTMENT   : Physics

TITLE OF DISSERTATION   : Effect of Brown's Gas Enriched Hydrocarbon Combustion on Engine Emissions and Performance

DATE OF PAYMENT OF   : 27$^{th}$ July, 2012

APPROVAL OF RESEARCH PROPOSAL   :

1. BPGS/BOS   : 15.05.2013

2. SCHOOL BOARD   : 20.05.2013

  REGISTRATION NO. & DATE   : MZU/Ph.D./518 of 20.05.2013

  EXTENSION   : 2 YEARS

## BIODATA

| | | |
|---|---|---|
| **Name** | : | J. Lalnunthari |
| **Father's Name** | : | J. Lalzaua |
| **Address** | : | K-23, Parallel Road, Bazar Veng, Lunglei, Mizoram; India-796701 |
| **Subject of Specialization** | : | Electronics |
| **Date of Birth** | : | 7$^{th}$ November 1988 |

**Educational Qualifications:**

- **HSLC**      2004      Distinction

- **HSSLC**      2006      First Division

- **B.Sc (Physics)**      2009      First Division

- **M.Sc (Physics)**      2011      First Division

- **Pre-Ph.D**      2013      Grade O

**Research Experience:**

- Completed M.Sc Project work on FPGA Based Controller of Traffic.
- Started research works in Fuel Energy and Hydrogen Energy under the supervision of Dr. Hranghmingthanga, Department of Physics, Mizoram University, Aizawl, Mizoram since May 2013 till date.
- Characterization of HHO Dry Cell on its Thermodynamics Aspects and its Electrical Efficiency of Electrolysis.
- Mileage Measurement of Maruti 800 with newly develops Voltage Drop Method, Linear and Polynomial Resistance Method.
- Studied the effect of HHO gas on the performance and emissions characteristic on Spark Ignition Engine.